Crystal and molecular structure of phosphetane oxides
by James Allen Campbell

A thesis submitted in partial fulfillment of the requirements for the degree of MASTER OF SCIENCE in Chemistry
Montana State University

Abstract:
Tho crystal and molecular structures of two phosphetane oxides were solved hy x-ray diffraction.

2,2,3-trimethyl-1-phenylphosphetane 1-oxide (C12POH17) crystallizes in space group P21/c with a = 10.582 Å, b = 12.680 Å, c = 10.299 Å, β= 119.03°. The phenyl group is planar, but the four-membered ring is puckered to some degree. The final R is 4.790 for 997 observed reflections.

2,2,3,4,4-pentamethyl-1-t-butylphosphetane 1-oxide (C12POH25) crystallizes in space group P21 with a = 6.133 Å, b = 12.174 Å, c = 9.047 Å, β = 96.42°. Since the refinement did not converge, only the gross structure is presented here.

STATEMENT OF PERMISSION TO COPY

In presenting this thesis in partial fulfillment of the requirements for an advanced degree at Montana State University, I agree that the Library shall make it freely available for inspection. I further agree that permission for extensive copying of this thesis for scholarly purposes may be granted by my major professor, or, in his absence, by the Director of Libraries. It is understood that any copying or publication on this thesis for financial gain shall not be allowed without my written permission.

Signature James A. Campbell

Date Aug. 7, 1974

CRYSTAL AND MOLECULAR STRUCTURE OF PHOSPHETANE OXIDES

by

James Allen Campbell

A thesis submitted in partial fulfillment
of the requirements for the degree

of

MASTER OF SCIENCE

in

Chemistry

Approved:

Chairman, Examining Committee

Head, Major Department

Graduate Dean

MONTANA STATE UNIVERSITY
Bozeman, Montana

August, 1974

ACKNOWLEDGMENT

I wish to thank Dr. Charles N. Caughlan for his advice and guidance and other members of the faculty of Montana State University for their help.

I wish to especially thank Dr. G. D. Smith for his advice and assistance.

Finally, I wish to thank my wife, Marty, for her patience, understanding, and support while this research was being completed.

TABLE OF CONTENTS

	Page
LIST OF TABLES	vi
LIST OF FIGURES	vii
ABSTRACT	ix
INTRODUCTION	1
PART I	
2,2,3-TRIMETHYL-1-PHENYLPHOSPHETANE 1-OXIDE	
I. The Crystal and Molecular Structure	2
Introduction	3
Preparation of the crystals	7
Density of the compound	7
Determination of space group and cell parameters	7
Collection of the data	8
Treatment of the data	10
Structure determination and refinement	13
Discussion of the structure	19
PART II	
2,2,3,4,4-PENTAMETHYL-1-t-BUTYLPHOSPHETANE 1-OXIDE	
I. Crystal and Molecular Structure	56
Introduction	57
Choice of crystal	58
Density of compound	59

Determination of space group and cell dimensions 61

Data collection 63

Treatment of data 63

Determination of structure 63

Refinement 65

Discussion of structure 66

SUMMARY AND CONCLUSIONS 71

BIBLIOGRAPHY 73

LIST OF TABLES

PART I

Page

2,2,3-TRIMETHYL-1-PHENYLPHSOPHETANE 1-OXIDE

TABLE I Crystal Data 9

TABLE II Positional Parameters of Non-hydrogen Atoms 20

TABLE III Anisotropic Thermal Parameters of Non-hydrogen Atoms . 21

TABLE IV Hydrogen Atom Parameters 23

TALBE V Observed and Calculated Structure Factors 25

TABLE VI Least-squares Plane 39

TABLE VII Bond Distances for Half-normal Probability Plot . . . 41

PART II

2,2,3,4,4-PENTAMETHYL-1-t-BUTYLPHOSPHETANE 1-OXIDE

TABLE VIII Crystal Data 62

TABLE IX Positional Parameters of Non-hydrogen Atoms 67

LIST OF FIGURES

PART I

Page

2,2,3-TRIMETHYL-1-PHENYLPHOSPHETANE 1-OXIDE

FIGURE I — Previous Structures of Phosphetane Oxides . . . 4

FIGURE II — Structure (Hydrogens not included) 29

FIGURE III — Structure (Hydrogens included) 30

FIGURE IV — Structure (Puckering in four-membered ring) . . 31

FIGURE V — Bond Angles 32

FIGURE VI — Bond Distances 33

FIGURE VII — Comparison of Ring Pucker in Four Structures . 35

FIGURE VIII — Normal Probability Plot 38

FIGURE IX — Half-normal Probability Plot for Bond Distances in Two Unsymmetrical Phosphetane Oxides 46

FIGURE X — Structure of Previous Unsymmetrical Phosphetane Oxide 47

FIGURE XI — Mechanism for Basic Hydrolysis 49

FIGURE XII — Mechanism for Reduction with Hexachlorodisilane 53

FIGURE XIII — Stereoscopic Packing Diagram 54

FIGURE XIV — Stereoscopic Diagram 55

PART II

2,2,3,4,4-PENTAMETHYL-1-t-BUTYLPHOSPHETANE 1-OXIDE

FIGURE XV — Graphical Illustration of "Whipple Disc" . . . 60

FIGURE XVI — Molecular Structure 68

FIGURE XVII Bond Angles 69

FIGURE XVIII Bond Distances 70

ABSTRACT

The crystal and molecular structures of two phosphetane oxides were solved by x-ray diffraction.

2,2,3-trimethyl-1-phenylphosphetane 1-oxide ($C_{12}POH_{17}$) crystallizes in space group $P2_1/c$ with a = 10.582 Å, b = 12.680 Å, c = 10.299 Å, β = 119.03°. The phenyl group is planar, but the four-membered ring is puckered to some degree. The final R is 4.790 for 997 observed reflections.

2,2,3,4,4-pentamethyl-1-t-butylphosphetane 1-oxide ($C_{12}POH_{25}$) crystallizes in space group $P2_1$ with a = 6.133 Å, b = 12.174 Å, c = 9.047 Å, β = 96.42°. Since the refinement did not converge, only the gross structure is presented here.

INTRODUCTION

This dissertation is divided into two parts, each presenting a different crystal structure which makes significant contributions to the literature. The first, that of 2,2,3-trimethyl-1-phenyl-phosphetane 1-oxide has yielded information concerning the geometry of the four-membered ring and the conformation of the phosphorus hetereocyclic ring.

The second, that of 2,2,3,4,4-pentamethyl-1-t-butylphosphetane 1-oxide was investigated to assist in understanding the kinetic data. A study of the partial structure has yielded information concerning the bonding at the phosphorus atom.

PART I

2,2,3-TRIMETHYL-1-PHENYLPHOSPHETANE 1-OXIDE

CHAPTER I

THE CRYSTAL AND MOLECULAR STRUCTURE OF 2,2,3-TRIMETHYL-1-PHENYLPHOSPHETANE 1-OXIDE

INTRODUCTION

The determination of the three-dimensional structure of 2,2,3-trimethyl-1-phenylphosphetane 1-oxide is important for a number of reasons. X-ray analysis was undertaken to determine the structure and stereochemistry, and to understand the bonding at the phosphorus atom and the conformation of the phosphorus heterocyclic ring. It is of particular interest to the organophosphorus chemists to relate the structure to its reactivity. Examples of other structures of this series that have been done in this laboratory are shown in Figure I.

Of the previously reported structures, two are symmetrical and the other is an unsymmetrical phosphetane oxide. This is only the second unsymmetrical phosphetane oxide whose structure has been determined. Dr. Sheldon Cremer of Marquette University synthesized the compound and supplied the sample.

Phosphetane 1-oxides have been prepared by (a) the reactions of $Me_3CCH{=}CR^1R^2$ with $RPCl_2$ in the presence of a Fridel-Crafts catalyst, followed by hydrolysis of the complex; or (b) reaction of 2,2,3,4,4 pentamethyl trimethylenephosphinic acid chloride with a Grignard reagent, RMgBr, followed by hydrolysis of the product (5).

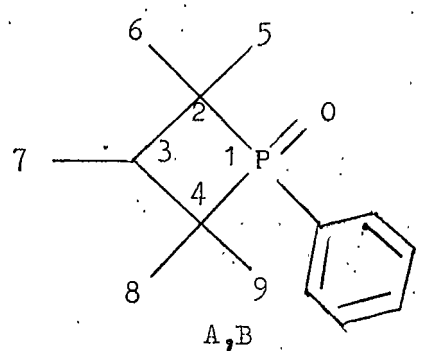

A,B

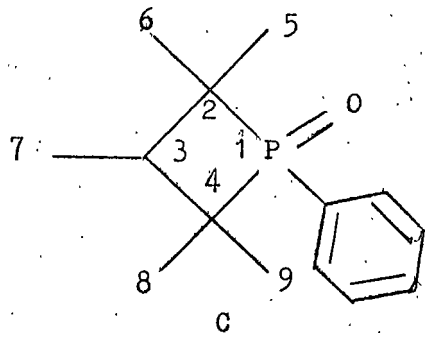

C

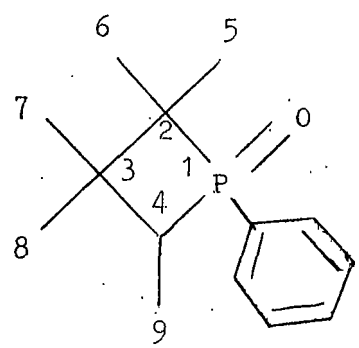

D

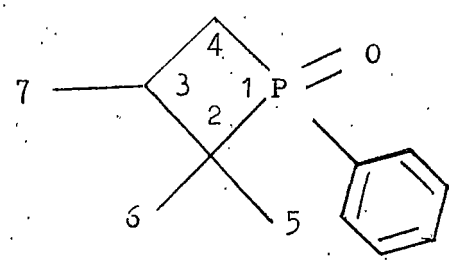

E

FIGURE I

PHOSPHETANE 1-OXIDES FOR WHICH THREE-DIMENSIONAL STRUCTURES HAVE BEEN DETERMINED. A,B: METHYL-7 TRANS TO PHENYL (11) C: METHYL-7 CIS TO PHENYL (12) ; D: (10); E: THIS WORK

NUMBERS 5-9 INDICATE METHYL GROUPS

The 1-phenylphosphetane oxides show remarkable stability when subjected to hydrolysis under basic conditions. Corfield has reported the following two reactions (4):

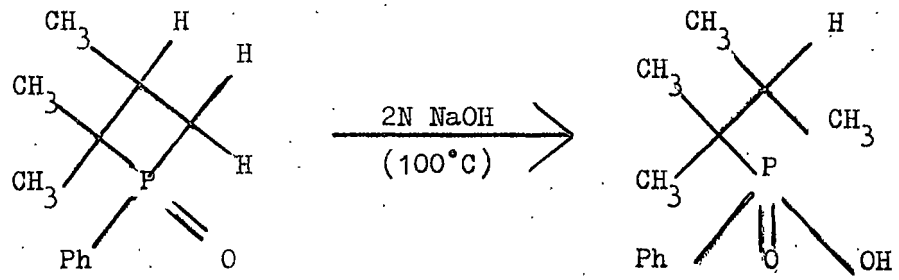

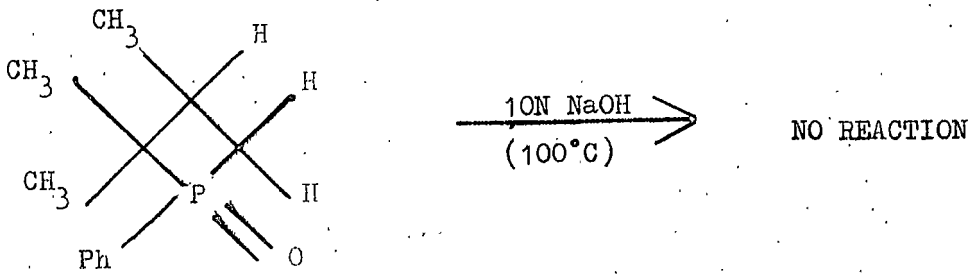

Ezzel has observed that the P-C bond can be cleaved by fusion with sodium hydroxide (7):

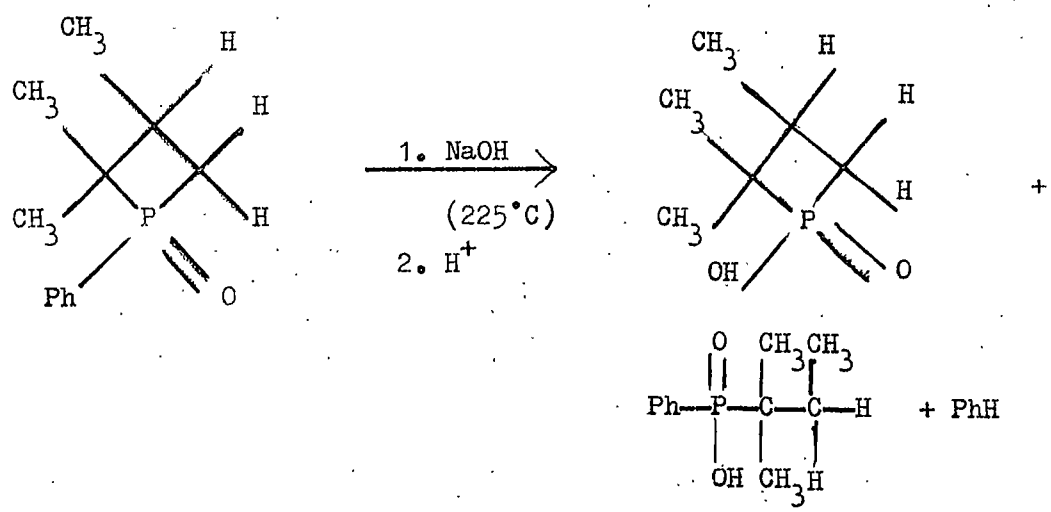

These reactions show the influence of α-substitution on the reactivity of the compounds. Clearly the direction of cleavage for the four-membered ring is influenced by both the ring and the stability of the leaving carbanion. The fact that the ring influences the direction of cleavage is in contrast to the saturated five-membered ring (8), but in agreement with the unsaturated five-membered ring (9).

Cremer and Chorvat observed that the reduction of phosphetane 1-oxides with $HSiCl_3$-$(C_2H_5)_3N$ proceeded with retention of configuration (1), in contrast to the inversion observed in the reduction of analogous acyclic phosphine oxides (14). Neither the mechanism of the reduction nor the rationale was at that time (1967) recognized.

Moret and Trefonas suggested that the 1-2 bond in the symmetrically substituted phosphetane oxides was equivalent to the 1-4 bond and that no preference was shown in the ring opening reactions (23). Ring opening reactions were favored at the 1-2 bond in preference to the 1-4 bond if the ring was unsymmetrically substituted. They also suggested that the 1-4 bond (bond to the greater substituted α-carbon) was shorter than the 1-2 bond (bond to the less substituted α-carbon). This was based on the fact that the longer, weaker bond would be easier to break. Solution of this structure and comparison of it with the previously determined unsymmetrically substituted phosphetane oxide should adequately answer that question.

PREPARATION OF CRYSTALS

The solid was dissolved in cyclohexane, and then the solvent was allowed to evaporate very slowly by placing a Petri dish of the solution in a dessicator. Two or three weeks were generally required for crystal growth to occur. One of the largest crystals was selected for the data collection. The crystal was sealed in a capillary tube, since the crystals turned opaque after prolonged exposure to the atmosphere. During data collection the crystal appeared to sublime.

DENSITY OF THE COMPOUND

The density of the compound was determined by flotation in a mixture of methanol and methyl iodide. The observed density was 1.14 g/cc., and the calculated density, assuming four molecules per unit cell, was 1.15 g/cc.

DETERMINATION OF SPACE GROUP AND CELL PARAMETERS

The crystal was mounted coincident with the a-axis. Weissenberg and precession photographs showed the following conditions for reflection:

hkl : no conditions

$0k0$: $k = 2n + 1$

$h0l$: $l = 2n + 1$

These extinctions uniquely determine the space group as $P2_1/c$.

The unit cell dimensions were determined by least squares refinement of the 2θ values of twenty general reflections using a General Electric XRD-5 diffractometer equipped with a General Electric single crystal orienter. The crystal data are listed in Table I.

COLLECTION OF THE DATA

The unique intensity data were collected by the θ-2θ scan method to $2\theta = 40^{\circ}$, using zirconium-filtered MoKα ($\lambda = .71069$ Å) radiation. The General Electric XRD-5 diffractometer used was equipped with a General Electric single crystal orienter, a scintillation counter, and a pulse height discriminator. Each reflection was scanned over an angular width of 2.0° per minute and background radiation was counted for ten seconds at each end of the 2θ scan. The take-off angle was set at 4.0°. The intensities of the $\bar{2}41$, 122, $\bar{2}21$ reflections were monitored during the data collection so that corrections could be made for such things as variations in room temperature, voltage supply, instrumental stability, and also to check for the possibility of decomposition of the crystal during the course of the data collection. A scale factor was calculated for each block of data using these standard reflections. A set of standard reflections was collected every hour throughout the entire data collection. The average value of the scale factor over the entire data collection was .996 with a standard deviation of .003. This value indicated that practically

TABLE I

CRYSTAL DATA

2,2,3-TRIMETHYL-1-PHENYLPHOSPHETANE 1-OXIDE

$C_{12}PH_{17}O$ F.W. 208.35 F(000)=448

MONOCLINIC, SPACE GROUP $P2_1/C$

a = 10.582(7)

b = 12.680(7)

c = 10.229(4)

β = 119.03(4)

Volume of unit cell	1200.42 $Å^3$
Molecules/unit cell	4
Linear absorption Coefficient (μ)	2.01 cm^{-1}
D_{calc}	1.150 g/cc
D_{meas}	1.140 g/cc
λ for MoK_α	.71069 Å

DIMENSIONS OF CRYSTAL

.630 X .378 X .315mm

no decomposition of the crystal occured during the data collection.

TREATMENT OF THE DATA

Structure factors ($|F_o|$) were calculated using the usual Lorentz-polarization correction for diffractometer data. The weights were calculated for each reflection assuming Poisson counting statistics and a correction factor, k_2, corresponding to the instability of the instrument. The appropriate weight of an observation is given by the reciprocal of the variance (σ^2) of the observation where σ is the standard deviation.

$$w = \frac{1}{(\sigma_F)^2}$$

For diffractometer data, the standard deviation in the counts is

$$\sigma_{count} = \sqrt{N}$$

where

N = total number of counts

In measuring X-ray reflections, the background count must always be considered. If the background has been measured on either side of the reflection for one half the time used in counting the peak, then the net peak count is

$$N_{pk} = N_T - nN_{bg1} - nN_{bg2}$$

where N_T is the total peak count, N_{bg1} and N_{bg2} are the background counts on either side of the peak, and n is the number needed to bring the background times equal to $\frac{1}{2}$ the time used in counting the peak. In this particular case, the backgrounds were counted for ten seconds on each side of the peak and the peak was counted for one minute. As a result, n would equal three. The standard deviation in N_{pk} is given by the following ezpression:

$$\sigma_{pk} = \sqrt{N_T - n^2 N_{bg1} - n^2 N_{bg2}}$$

This expression is the estimated uncertainty due only to statistical fluctuations in the counting. An additional uncertainty must be included to allow for instrumental instability. This can be determined from the standard reflections which are measured periodically and is usually in the range of .01 - .03. Inclusion of the machine stability yields a final expression for the standard deviation in the relative intensity

$$\sigma_{I_{rel}} = \sqrt{\sigma_{pk}^2 + (k_2 N_{pk})^2}$$

where

k_2 = the machine stability constant

The standard deviation in F can then be derived from the equation

$$F = \frac{k}{\sqrt{Lp}} \sqrt{I_{rel}}$$

where

L = the Lorentz factor

p = the polarization factor

The polarization correction is a function of the diffraction angle, and is given by the following expression: (28)

$$p = \left[1 + \cos^2 2\theta \right] /2$$

The Lorentz correction is defined by the following equation: (28)

$$L = \frac{1}{2\cos\theta} \sqrt{\cos^2\mu - \cos^2\theta}$$

The Lorentz correction is a function of the Bragg angle θ as well as the equi-inclination Weissenberg technique. The diffractometer data taken in the laboratory must be corrected using an equi-inclination angle of zero. When these corrections are applied the intensities are converted to observed structure factors. The conversion is given by

$$\left| F(hkl) \right|^2 = KI/Lp$$

where K = the scale factor.

The standard deviation is then determined from $\sigma_{I_{rel}}$ and the relationship between I_{rel} and F. This expresssion is given by the following expression (27)

$$\sigma_F = \frac{k}{\sqrt{Lp}} \frac{1}{2} \sqrt{\frac{N_T + n^2 N_{bg1} + n^2 N_{bg2} + (k_2 N_{pk})^2}{N_{pk}}}$$

where k_2 = the scale constant.

The data set consisted of 1215 reflections of which 997 were considered observable at the two sigma level. The instrumental instability constant was set at .04. Scattering factor curves were taken from the International Tables (15), as were the anamolous scattering corrections (Δ f' and Δ f") for phosphorus. The scattering factor curve for hydrogen was taken from Stewart, et al (25).

STRUCTURE DETERMINATION AND REFINEMENT

The phosphorus atomic positions were easily located from a three-dimensional Patterson map. The Patterson map is a representation of all the interatomic distances translated back to the origin. The Patterson function is given by the following expression (2)

$$P(UVW) = \sum_h \sum_k \sum_l (F_{hkl})^2 \exp(A)$$

$$A = -2\pi i(hU + kV + lW)$$

where

$P(UVW)$ = the value of the Patterson function at the coordinates U,V,W

$F(hkl)^2$ = is the observed value of the square of the structure factor

V_c = the volume of the unit cell

h,k,l = are the Miller indices

U,V,W = are the interatomic vectors

The Patterson function for a monoclinic crystal system with the b axis designated as the unique axis is (16)

$$P(UVW) = \frac{4}{V_c} \sum_0^\infty \sum_0^\infty \sum_0^\infty \left(|F(hkl)|^2 \cos 2\pi (hU + lW) + |F(\bar{h}kl)|^2 \cos 2\pi (hU - lW) \right) \cos 2\pi kV$$

For the crystal symmetry $P2_1/c$, the following equivalent positions exist:

$$x \ , \ y \ , \ z$$

$$-x \ , \ -y \ , \ -z$$

$$-x \ , \ \tfrac{1}{2} + y \ , \ \tfrac{1}{2} - z$$

$$x \ , \ \tfrac{1}{2} - y \ , \ \tfrac{1}{2} + z$$

Considering the vectors between an atom at (x,y,z) and $(-x, \frac{1}{2} + y, \frac{1}{2} - z)$ the following is obtained $u=2x$, $v=\frac{1}{2}$, $w=\frac{1}{2} + 2z$ indicating that a Harker section exists at $v=\frac{1}{2}$ due to the 2_1 screw axis in the y

direction. Due to the other symmetry transformations of the equivalent atoms, the following vectors also arise 2x, 2y, 2z due to the center of symmetry, and 0, $\frac{1}{2} \pm 2y$, $\frac{1}{2}$, due to the c glide. This last vector unit is termed the Harker line.

The atomic coordinates for the phosphorus atom were determined from the Harker plane and the Harker line. The major peak was found at (.195, .111, .179). These coordinates were used to generate the first Fourier map.

A three-dimensional Fourier map was first synthesized from the calculated signs of the structure factors applied to the observed value of the first phosphorus atomic positons. The electron density throughout the cell is given by the following expression (26)

$$\rho(X,Y,Z) = \frac{1}{V_c} \sum_h \sum_k \sum_l F_{hkl} \exp(A)$$

$$A = -2\pi i(hX + kY + lZ)$$

where

$\rho(XYZ)$ = is the electron density expression at the coordinates X,Y,Z

V_c = the volume of the unit cell

F_{hkl} = the value of the observed structure factors

The Fourier map is used to obtain and locate atomic positions. The Fourier series requires correct knowledge of the phases as well as the amplitudes for the correct location of the atomic positions.

The atomic parameters may be in considerable error if some incorrect phases are used. However, erroneous phases and amplitudes may give correct atomic positions.

The Fourier expression for the space group $P2_1/c$ is as follows(16)

$$\rho(XYZ) = \frac{4}{V_c} \left(\sum_0^\infty \sum_0^\infty \sum_0^\infty {}^{k+l=2n} [F(hkl) \cos 2\pi (hX + lZ) + F(\bar{h}kl) \cos 2\pi (-hX + lZ)] \cos 2\pi kY - \sum_0^\infty \sum_0^\infty \sum_0^\infty {}^{k+l=2n+1} [F(hkl) \sin 2\pi (hX + lZ) + F(\bar{h}kl) \sin 2\pi (-hX + lZ)] \sin 2\pi kY \right)$$

From the first Fourier map, it was possible to locate the atoms of the four-membered ring. The remaining atomic positions were revealed by five subsequent Fourier maps. R was then 21.2% and the bond angles and bond distances were reasonable to start refinement.

Full matrix least squares refinement of the positional and isotropic thermal parameters for the fourteen heavy atoms produced an R value of .091 (3). A series of difference Fourier maps were needed to determine the positions of all the hydrogen atoms. All seventeen hydrogen atoms were located from several difference maps.

In the case of the difference Fourier map, the coefficients are the Δ F's, i.e. the quantities $F_o - F_c$, calculated on the basis of some model. The Δ F's and the Fourier calculated from them are obviously related to the errors in the model as compared to the true structure.

Finally, the positional and individual anisotropic thermal parameters of the fourteen non-hydrogen atoms were refined. Also included in this refinement were the positional and isotropic temperature factors for the seventeen hydrogen atoms. At the completion of refinement R=.047. The largest shift divided by the standard deviation at this point of refinement was less than .2.

A final difference map was calculated to make sure that all of the atoms had been located and to determine if molecules of solvent were present. The largest peaks on this map were $\pm$ .25 and were found close to the phosphorus atom.

Refinement is taken to mean least squares refinement, where the quantity commonly minimized is

$$D = \sum_{hkl} w_{hkl} \left(|F_o| - \left| \frac{1}{k_1} F_c \right| \right)^2$$

where

w_{hkl} = weight of the observation

$\sum_{hkl}$ = summation over all observed relections

There are several indicators which describe the fit of the model to the data or the probable correctness of the model used. The first of these is the residual index (sometimes referred to as the reliability index) R, defined as:

$$R_{obs} = \frac{\sum |\Delta F|}{\sum |F_o|} = \frac{\sum \left| |F_o| - |F_c| \right|}{\sum |F_o|}$$

This expression is for only the observed data. The R value is by no means the perfect guide to this correctness of fit.

The residual index for the total data set is given by the following expression:

$$R_{obs + unobs} = \frac{\sum \left| |F_o| - |F_c| \right|}{\sum |F_o|}$$

Hamilton considered the question of identifying meaningful changes in R produced when the model is altered. Instead of the conventional R, he defined a weighted residual (13)

$$R'' = \left\{ \frac{\sum w_i \left(|F_{o_i}| - |F_{c_i}| \right)^2}{\sum w_i |F_{o_i}|^2} \right\}^{\frac{1}{2}}$$

Another indicator is the standard deviation in an observation of unit weight

$$S = \left[\frac{\sum w(\left| F_o \right| - \left| F_c \right|)^2}{m - n} \right]^{\frac{1}{2}}$$

where

m = the number of observations

n = the number of variables refined in the model

DISCUSSION OF THE STRUCTURE

The positional parameters of the non-hydrogen atoms are listed in Table II. The thermal parameters of the non-hydrogen atoms are listed in Table III. The hydrogen atom parameters are listed in Table IV. The calculated and observed structure factors are listed in Table V.

Figure II shows an Ortep drawing of the structure without the hydrogen atoms and Figure III is an Ortep drawing of the structure including the hydrogen atoms. Figure IV is an Ortep drawing of the entire structure showing the pucker in the four-membered ring with the ellipsoids calculated at the 50% probability level (19). The bond angles are presented in Figure V and the bond distances are shown in Figure VI.

The Ortep drawing clearly shows that the single methyl group is trans to the phenyl group. Figure VI shows that the two P-C bonds differ by about ten standard deviations. Moret and Trefonas (23) have suggested that the P-C bond to the least substituted α-carbon

TABLE II

POSITIONAL PARAMETERS FOR THE NON-HYDROGEN ATOMS IN 2,2,3-TRIMETHYL-1-PHENYLPHOSPHETANE 1-OXIDE

ATOM	x/a	y/b	z/c
P	.19286(12)[a]	.10972(9)	.17427(12)
C(2)	.1710(4)	.0479(3)	.3243(5)
C(3)	.0523(5)	.1306(4)	.1940(5)
C(4)	.0222(4)	.1631(3)	.1369(4)
C(5)	.1100(5)	-.0639(3)	.2777(6)
C(6)	.2955(5)	.0472(4)	.4807(5)
C(7)	-.0825(6)	.0969(4)	.2993(6)
C(8)	.3294(4)	.2105(3)	.2540(4)
C(9)	.4577(5)	.1929(3)	.2562(5)
C(10)	.5676(6)	.2672(5)	.3165(7)
C(11)	.5483(6)	.3565(4)	.3769(6)
C(12)	.4211(6)	.3768(4)	.3745(6)
C(13)	.3119(5)	.3034(3)	.3146(6)
O	.2104(2)	.0459(2)	.0639(3)

[a]The number in parentheses is the standard deviation and refers to the least significant digits.

TABLE III

ANISOTROPIC THERMAL PARAMETERS FOR THE NON-HYDROGEN ATOMS IN

2,2,3-TRIMETHYL-1-PHENYLPHOSPHETANE 1-OXIDE

ATOM	β_{11}	β_{22}	β_{33}	β_{12}	β_{13}	β_{23}
P	.0109(2)	.0053(1)	.0131(1)	-.0001(1)	.0061(1)	-.0007(1)
C(2)	.0137(6)	.0058(3)	.0138(7)	-.0009(4)	.0058(6)	-.0004(4)
C(3)	.0155(7)	.0084(4)	.0165(8)	-.0017(5)	.0108(6)	-.0023(4)
C(4)	.0127(7)	.0058(3)	.0172(8)	-.0001(4)	.0074(5)	-.0013(4)
C(5)	.0190(8)	.0077(4)	.0222(9)	-.0025(5)	.0111(7)	-.0003(5)
C(6)	.0214(9)	.0099(4)	.0149(8)	-.0041(5)	.0064(8)	.0010(5)
C(7)	.0238(10)	.0133(5)	.0319(11)	-.0017(6)	.0210(9)	-.0028(7)
C(8)	.0103(6)	.0066(4)	.0136(7)	-.0008(4)	.0061(5)	.0007(4)

e.s.d.'s are in parentheses

The expression for the anisotropic thermal parameters is of the form:

$$\exp(-\beta_{11}h^2 - \beta_{22}l^2 - \beta_{33}k^2 - 2\beta_{12}hk - 2\beta_{13}hl - 2\beta_{23}kl)$$

TABLE III (CONTINUED)

ANISOTROPIC THERMAL PARAMETERS FOR THE NON-HYDROGEN ATOMS IN

2,2,3-TRIMETHYL-1-PHENYLPHOSPHETANE 1-OXIDE

ATOM	β_{11}	β_{22}	β_{33}	β_{12}	β_{13}	β_{23}
C(9)	.0152(8)	.0071(4)	.0217(9)	-.0005(5)	.0097(7)	-.0009(4)
C(10)	.0126(8)	.0119(6)	.0312(12)	-.0022(6)	.0170(8)	-.0002(7)
C(11)	.0176(9)	.0087(5)	.0223(10)	-.0069(6)	.0064(7)	-.0019(6)
C(12)	.0194(9)	.0089(4)	.0216(9)	-.0044(6)	.0107(7)	-.0034(6)
C(13)	.0153(7)	.0066(4)	.1203(8)	-.0036(5)	.0104(6)	-.0040(5)
O	.0137(5)	.0075(2)	.0161(5)	-.0005(2)	.0079(4)	-.0036(3)

e.s.d's are in parentheses.

The expression for the anisotropic thermal parameters is of the form:

$$\exp(-\beta_{11}h^2 - \beta_{22}l^2 - \beta_{33}k^2 - 2\beta_{12}hk - 2\beta_{13}hl - 2\beta_{23}kl)$$

TABLE IV

HYDROGEN ATOM POSITIONS AND ISOTROPIC THERMAL PARAMETERS

FOR 2,2,3-TRIMETHYL-1-PHENYLPHOSPHETANE 1-OXIDE

ATOM	x/a	y/b	z/c	B_{iso}
H(1)	.099(4)[a]	.186(3)	.364(4)	5.4(9)
H(2)	-.051(4)	.125(3)	.060(4)	4.4(8)
H(3)	.010(3)	.2311(2)	.116(3)	2.7(6)
H(4)	.471(3)	.133(2)	.223(3)	4.2(8)
H(5)	.658(4)	.244(3)	.3254(4)	7.(1)
H(6)	.601(4)	.405(3)	.407(4)	5.1(9)
H(7)	.409(3)	.433(2)	.447(3)	8.3(7)
H(8)	.210(3)	.318(3)	.329(3)	7.8(7)
H(9)	.375(5)	-.008(4)	.489(5)	10.(1)
H(10)	.273(4)	.024(3)	.548(5)	6.(1)
H(11)	.329(3)	.114(3)	.506(3)	4.3(7)

[a]The number in parentheses is the standard deviation and refers to the least significant digits.

TABLE IV (CONTINUED)

HYDROGEN ATOM POSITIONS AND ISOTROPIC THERMAL PARAMETERS

FOR 2,2,3-TRIMETHYL-1-PHENYLPHOSPHETANE 1-OXIDE

ATOM	x/a	y/b	z/c	B_{iso}
H(12)	.184(4)[a]	-.103(3)	.273(4)	6.1(9)
H(13)	.028(3)	-.065(2)	.169(3)	4.8(8)
H(14)	.073(5)	-.091(3)	.344(5)	8.(1)
H(15)	-.150(3)	.160(2)	.280(4)	9.1(7)
H(16)	-.113(5)	.127(3)	.251(5)	9.(1)
H(17)	-.061(3)	.094(3)	.394(4)	6.7(7)

[a]The number in parentheses is the standard deviation and refers to the least significant digits.

TABLE V

CALCULATED AND OBSERVED STRUCTURE FACTORS

L= 0 H= 0		
K	FO	FC
4	58	61
6	24	22
10	5	5
12	18	18

L= 0 H= 1		
K	FO	FC
0	21	21
1	83	82
2	62	65
3	52	53
4	35	36
5	13	13
6	13	13
11	22	22

L= 0 H= 2		
K	FO	FC
1	3	4
2	48	53
3	7	7
5	7	7
6	20	21
7	12	12
9	15	15
10	9	9
12	9	10

L= 0 H= 3		
K	FO	FC
0	30	30
1	32	31
2	41	39
3	36	36
4	28	27
5	35	34
6	20	19
8	10	10

L= 0 H= 4		
K	FO	FC
0	7	7
1	3	1
2	4	4
3	61	60
5	9	9
6	12	12
7	16	16
9	4	2
11	11	11

L= 0 H= 5		
K	FO	FC
0	28	28
1	4	5
2	11	10
3	4	3
4	20	20
5	8	10
6	8	8
7	7	7
8	15	15

L= 0 H= 6		
K	FO	FC
0	11	13
1	17	17
3	26	26
7	12	13
9	7	7

L= 0 H= 7		
K	FO	FC
0	8	5
1	25	25
2	10	11
3	13	13
4	9	9
6	8	7
8	5	5

L= 0 H= 8		
K	FO	FC
0	31	33
3	6	5
4	9	10

L= 0 H= 9		
K	FO	FC
0	8	7
1	6	6

L= 1 H= 0		
K	FO	FC
1	29	29
2	75	78
3	47	48
4	6	6
5	9	9
6	10	11
7	8	7
8	6	7
9	6	7
10	11	11
12	13	12

L= 1 H= 1		
K	FO	FC
1	73	74
1	63	62
2	87	90
2	43	44
3	19	19
3	9	9
4	7	7
5	30	30
5	13	13
6	38	37
6	26	25
7	6	7
7	9	9
8	4	5
8	11	10
9	13	13
9	7	7
10	15	14
10	7	6
11	7	8
12	8	6
12	4	5

L= 1 H= 2		
K	FO	FC
1	43	42
1	49	53
2	36	37
3	15	13
3	4	4
4	23	22
4	59	57
5	38	38
5	25	24
6	4	6
7	4	4
7	10	10
8	8	8
8	9	9
9	9	8
9	7	6
10	11	12
10	15	15
11	4	5
12	5	3

L= 1 H= 3		
K	FO	FC
1	21	21
1	39	38
2	26	25
2	14	14
3	10	10
3	32	29
4	17	16
4	28	27
5	10	9
5	47	47
7	6	6
8	8	7
8	7	8
9	5	4
9	20	20
10	7	6
11	5	5

L= 1 H= 4		
K	FO	FC
1	41	41
1	23	23
2	4	5
2	39	37
3	11	11
3	6	6
4	18	18
4	28	28
5	10	10
5	14	16
6	4	4
6	8	7
7	5	4
7	9	9
8	4	3
9	8	6
9	15	14
10	9	8
10	4	5

L= 1 H= 5		
K	FO	FC
1	28	28
1	35	36
2	21	20
2	25	26
3	10	9
3	20	19
4	16	16
4	9	9
5	18	18
6	9	10
7	6	6
7	6	5
8	4	5
9	6	3

L= 1 H= 6		
K	FO	FC
1	12	12
1	17	18
2	30	30
3	12	12
4	9	9
4	8	8
5	9	9
5	19	19
7	5	6
7	6	7
9	11	10

L= 1 H= 7		
K	FO	FC
1	23	23
1	13	13
2	10	11
2	24	24
3	5	5
3	26	26
4	4	4
5	9	10
5	5	4
6	11	11
7	6	7
8	11	10

L= 1 H= -8		
K	FC	FC
1	10	10
2	13	13
2	13	13
3	8	9
4	15	14
5	4	3
6	12	12

L= 2 H= 0		
K	FO	FC
0	108	116
1	27	28
2	51	51
3	21	20
4	30	29
6	10	11
7	7	7
8	3	3
10	16	17
11	5	5
12	4	5

L= 2 H= 1		
K	FO	FC
0	45	47
1	27	27
1	85	88
2	54	55
2	44	46
3	23	23
3	21	20
4	48	47
4	12	12
5	12	12
5	46	46
7	8	8
7	19	19
8	22	22
8	9	9
9	13	12
10	4	1
10	11	11
11	11	12
11	15	15
12	4	1

L= 2 H= -2		
K	FO	FC
0	8	8
1	11	11
1	40	41
2	20	19
3	44	44
3	37	36
4	9	10
4	35	36
5	10	9
7	35	35
7	10	10
8	16	16
9	16	16
9	6	6
10	27	26
11	11	12
11	9	9

TABLE V (CONTINUED)

			C	11	11		1	12	11	K	FC	FC	L=	3 H=	3		3	12	12	L=	3 H=	-8		4	34	34
L=	2 H=	3	C	27	26		3	11	11	1	40	40		K	FC	FC	3	34	33		K	FC	FC	4	14	15
	K	FC	FC	1	17	17		4	5	4	2	14	15		1	12	12	4	4	5		1	8	7	5	4	4
	C	29	28	1	22	21		4	28	29	2	81	83		1	36	34	4	3	3		2	6	7	5	5	5
	C	17	18	2	5	5		5	5	5	3	15	16		2	14	15	5	16	16		3	18	18	6	16	15
	2	39	36	3	12	12		6	7	7	3	17	16		2	5	6	5	30	29		4	9	9	6	5	6
	3	17	17	3	22	21		8	14	14	4	8	7		3	12	12	6	14	14		7	7	5	7	14	14
	3	27	27	4	23	23		9	8	7	5	5	5		3	26	25	7	12	12					8	27	28
	4	24	25	5	4	4					6	29	27		4	10	11	8	8	8	L=	3 H=	-9	8	13	13
	5	13	13	5	24	24	L=	2 H=	-8		6	12	12		5	21	22	9	21	22		K	FC	FC	9	7	7
	6	16	15	6	7	7		K	FO	FC	7	7	7		6	11	12					1	4	3	10	8	7
	6	3	3	7	7	7		0	9	10	8	18	19		6	7	6	L=	3 H=	6		2	16	15	10	19	18
	7	4	4	7	5	6		1	4	0	8	14	15		7	5	5		K	FC	FC	3	4	2			
	7	33	35	8	4	4		2	16	18	9	9	9		7	21	21	1	9	7		5	5	5	L=	4 H=	2
	8	11	11	8	23	22		3	4	2	9	11	11		8	8	8	1	6	6		6	11	10		K	FC	FC
	9	10	11	9	4	2		7	13	13	10	8	8		9	17	17	2	8	8						0	5	8
	10	6	7	10	8	9					10	4	4		9	32	32	2	19	19	L=	3 H=	-10		0	16	16
	11	16	15				L=	2 H=	-9		11	4	5	10	9	10		3	5	3		K	FC	FC		1	7	8
				L=	2 H=	6		K	FO	FC	11	10	9	11	9	8		3	19	20		1	7	7		1	44	45
L=	2 H=	4		K	FO	FC		0	12	11								5	22	22		2	4	3		2	4	5
	K	FC	FC	0	24	25		1	6	3	L=	3 H=	2	L=	3 H=	4		6	5	6						2	16	17
	C	41	41	0	16	16		2	6	4		K	FO	FC		K	FO	FC	6	28	29	L=	4 H=	0		3	6	6
	C	23	24	1	6	6		5	7	8		1	15	14		1	7	6	7	10	11		K	FC	FC		3	22	21
	1	9	10	1	26	26						2	28	29		1	25	25	8	7	6		1	14	13		4	15	17
	1	26	23	2	13	14	L=	3 H=	0			2	10	9		2	11	11	9	14	15		3	17	17		4	30	29
	2	24	23	3	5	5		K	FO	FC		3	19	18		3	7	8	10	5	4		4	21	22		5	14	14
	3	26	26	3	28	29		1	26	26		4	4	5		6	23	23					5	19	20		5	9	8
	3	30	29	4	6	8		2	23	24		4	6	6		6	50	49	L=	3 H=	-7		6	4	4		7	27	27
	4	3	5	4	6	8		3	44	43		5	27	28		8	11	10		K	FO	FC	7	23	23		7	25	25
	4	21	22	5	7	7		4	28	28		5	6	6		8	19	18	1	6	5		8	15	15		8	5	9
	6	13	13	5	15	16		5	8	8		6	15	15		9	8	8	2	7	6		9	4	3		8	7	7
	7	4	4	7	28	29		6	21	20		7	7	7		10	9	9	2	12	12		11	4	5		10	18	19
	7	10	10	9	7	6		7	11	10		8	4	3		11	7	8	3	11	11						10	8	11
	8	14	18					8	12	11		8	25	24					4	10	10	L=	4 H=	1		11	11	11
	9	4	4	L=	2 H=	7		9	21	21		9	11	11	L=	3 H=	5		5	13	12		K	FC	FC			
	10	13	13		K	FO	FC	10	8	7		9	23	22		K	FO	FC	6	13	14		0	7	6	L=	4 H=	3
					C	7	7	11	5	5		10	4	3		1	13	12	7	4	4		1	11	10		K	FC	FC
L=	2 H=	5		C	20	20						11	7	6		2	4	4	8	14	13		2	25	23		0	9	9
	K	FC	FC	1	20	20	L=	3 H=	-1							2	4	5					3	31	32		0	7	6
	1	15	14	C	16	16		K	FO	FC	5	20	20		6	6	5	5	8	8	7	6	6	1	14	14

TABLE V (CONTINUED)

1	21	20	0	53	52	1	5	5	5	15	15	6	15	17	6	19	19	8	8	10	1	6	6
2	4	1	1	7	6	3	5	5	6	12	13	8	20	21	8	8	8				2	5	5
2	12	12	1	24	24	4	17	16	6	14	14	10	14	13				L=	6	H= 1	3	8	7
3	4	3	3	18	19	5	14	14	7	13	13				L=	5	H= -7	K	FC	FC	3	12	11
3	19	19	4	9	9	6	5	4	7	7	7	L=	5	H= 4	K	FC	FC	C	9	9	4	5	4
4	10	10	4	3	1	7	10	10	8	8	9	K	FC	FC	1	15	15	C	14	14	4	18	18
4	25	25	5	10	10	8	9	9	8	17	17	1	6	6	3	4	4	1	20	21	5	5	3
5	18	18	5	28	28				9	11	11	1	19	19	5	25	26	2	4	4	6	7	10
5	14	13	6	6	7	L=	4	H= -9	9	5	5	2	8	9	7	9	8	3	15	15	7	7	8
6	6	7	7	24	25	K	FO	FC				2	17	18				3	30	30	8	9	9
7	19	19	8	7	6	0	15	15	L=	5	H= 2	3	6	5	L=	5	H= -8	4	4	3	9	4	4
7	26	26	9	8	9	3	11	11	K	FC	FC	3	6	6	K	FC	FC	4	14	14			
8	17	17				4	9	8	1	3	2	4	4	2	1	9	9	5	7	7	L=	6	H= 4
9	6	4	L=	4	H= 6	5	5	6	1	28	28	4	16	16	2	15	15	5	19	19	K	FC	FC
9	8	8	K	FO	FC	6	14	13	2	17	17	5	17	18	3	6	6	6	5	5	0	10	10
10	7	8	0	5	5				3	8	8	6	14	14	4	14	15	6	5	5	0	26	26
11	9	9	1	10	10	L=	4	H=-10	3	49	49	6	15	15	5	6	7	7	8	8	1	7	6
			1	5	4	K	FO	FC	4	8	7	7	7	7	6	17	18	7	15	15	3	19	19
L=	4	H= 4	2	4	4	1	7	7	4	11	11	9	15	15	7	11	11	8	5	5	7	24	23
K	FO	FC	3	5	6	2	6	5	5	8	7							9	6	4			
0	16	18	3	10	9	3	7	6	5	15	15	L=	5	H= -5	L=	5	H= -9				L=	6	H= -5
0	9	8	4	22	22				6	20	21	K	FO	FC	K	FO	FC	L=	6	H= 2	K	FC	FC
1	11	10	6	4	7	L=	5	H= 0	7	7	7	1	20	20	2	18	19	K	FO	FC	0	17	17
2	12	11	7	20	20	K	FO	FC	7	6	6	2	12	12	3	5	4	C	13	13	1	17	16
2	30	29	8	4	4	1	22	21	8	13	13	2	8	7	5	9	8	C	15	15	2	3	1
3	7	8	10	11	10	3	9	8	9	21	22	3	3	2				1	7	7	3	22	22
3	11	12				4	11	11				4	4	3	L=	5	H=-10	1	25	26	4	7	7
4	15	16	L=	4	H= -7	6	19	20	L=	5	H= 3	5	29	29	K	FO	FC	3	13	13	5	6	6
4	24	24	K	FO	FC	9	14	14	K	FC	FC	6	7	7	1	11	12	4	11	9	7	4	3
5	4	5	0	12	11				1	7	6	8	5	5	2	5	3	5	3	0	8	8	7
7	17	17	1	4	3	L=	5	H= -1	2	5	3	9	9	9	3	6	8	7	4	4			
8	19	19	3	3	3	K	FO	FC	2	21	20							7	11	12	L=	6	H= -6
9	4	3	4	17	17	1	3	4	3	9	9	L=	5	H= -6	L=	6	H= 0	8	5	6	K	FC	FC
10	18	19	5	7	7	2	10	9	3	3	3	K	FO	FC	K	FO	FC				0	22	23
11	10	10	7	11	13	2	41	42	4	10	10	1	3	3	0	20	20	L=	6	H= 3	1	18	17
			8	10	10	3	7	7	4	6	5	2	14	14	2	5	6	K	FC	FC	2	21	21
L=	4	H= 5				3	7	7	5	16	15	3	4	5	3	12	12	0	4	4	4	9	8
K	FO	FC	L=	4	H= -8	4	17	16	5	6	6	4	12	12	4	17	17	0	21	20	5	13	13
6	7	8	1	5	3	L=	7	H= -4	4	16	16				4	22	22	K	FC	FC	K	FC	FC
7	7	6	2	20	19	K	FO	FC	6	15	15	L=	8	H= -3	5	4	1	1	6	7	0	6	4

TABLE V (CONTINUED)

8	5	4

L=	6	H= =7
K	FC	FC
C	10	10
1	7	7
2	6	6
3	17	16
4	18	18
7	5	3
8	9	8

L=	6	H= =8
K	FC	FC
C	29	29
1	5	3
2	8	8
4	16	15
6	8	9
7	7	7

L=	6	H= =9
K	FC	FC
C	25	24
1	11	11
2	4	4
4	7	7
5	5	4

L=	6	H=-10
K	FC	FC
C	9	8
1	7	8
3	8	8

L=	7	H= C
K	FC	FC

3	13	13
4	21	21
5	6	6
6	15	15
7	5	5

L=	7	H= 1
K	FC	FC
1	10	10
1	23	23
2	10	11
3	4	4
4	4	4
4	9	9
5	15	14
5	20	21
6	12	12
7	4	3

L=	7	H= =2
K	FC	FC
1	27	28
2	8	7
2	13	13
3	4	4
3	11	11
4	10	10
4	4	5

L=	7	H= 3
K	FC	FC
1	4	5
1	11	11
2	29	29
5	12	12
8	4	4

1	26	26
3	4	2
5	13	14
6	4	4
7	12	12
8	7	8

L=	7	H= =5
K	FC	FC
1	9	8
2	16	16
3	11	12
4	6	6
6	5	4
7	4	3
8	11	11

L=	7	H= =6
K	FC	FC
1	13	12
3	13	13
4	14	15
5	8	6

L=	7	H= =7
K	FC	FC
1	15	15
2	19	19
3	8	8
5	13	15
6	9	8

L=	7	H= =8
K	FC	FC
1	5	2
2	25	25
3	4	4

L=	7	H= =9
K	FC	FC
1	13	13
2	9	9
3	4	4

L=	7	H=-10
K	FC	FC
1	6	6

L=	8	H= C
K	FC	FC
C	8	8
1	7	6
2	9	8
3	4	3
5	10	10

L=	8	H= 1
K	FC	FC
C	13	12
2	10	10
3	4	4
5	16	17
4	12	12

L=	8	H= =2
K	FC	FC
C	26	27
1	9	10
3	7	7
4	14	15
5	4	5

K	FC	FC
C	21	20
1	12	12
2	7	7
3	9	9
7	8	8

L=	8	H= =4
K	FC	FC
C	6	8
1	5	5
3	14	15
4	5	6
5	5	6
6	8	8
7	6	4

L=	8	H= =5
K	FC	FC
1	9	9
4	7	7
C	15	15
2	10	10
3	8	7
6	12	13

L=	8	H= =6
K	FC	FC
C	7	7
1	12	11
2	4	5
3	12	14
4	4	4
7	9	8

L=	8	H= =7
K	FC	FC
0	26	26
3	6	6

6	4	3

L=	8	H= =8
K	FC	FC
0	15	14
1	8	7
3	14	14
4	9	9
5	6	4

L=	8	H= =9
K	FC	FC
1	9	9
3	6	8

L=	9	H= C
K	FC	FC
1	9	9
2	7	6

L=	9	H= =1
K	FC	FC
1	7	7
2	7	6

L=	9	H= =2
K	FC	FC
2	7	6

L=	9	H= =3
K	FC	FC
1	8	7
3	5	3
4	5	5
5	9	8

L=	9	H= =4

2	8	8
4	4	5

L=	9	H= =5
K	FC	FC
1	5	5
2	8	6
5	7	8

L=	9	H= =6
K	FC	FC
1	11	11
2	16	16
3	8	8
5	7	5

L=	9	H= =7
K	FC	FC
1	7	8
2	21	20
3	7	7
4	5	4

L=	9	H= =8
K	FC	FC
1	7	7

L=	10	H= C
K	FC	FC
1	6	4
3	6	6

L=	10	H= =4
K	FC	FC
0	8	8

L=	10	H= =5

1	6	7

L=	10	H= =6
K	FC	FC
C	13	13

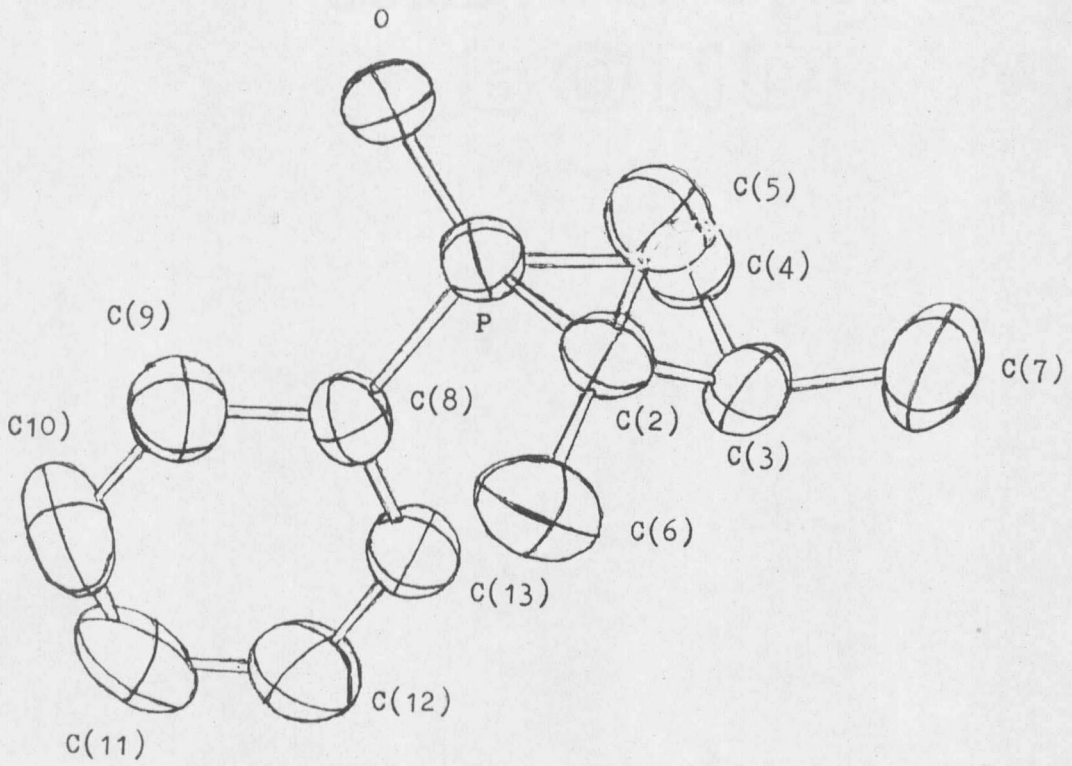

FIGURE II

MOLECULAR STRUCTURE OF
2,2,3-TRIMETHYL-1-PHENYLPHOSPHETANE 1-OXIDE
AT THE 50% PROBABILITY LEVEL (HYDROGENS NOT INCLUDED)

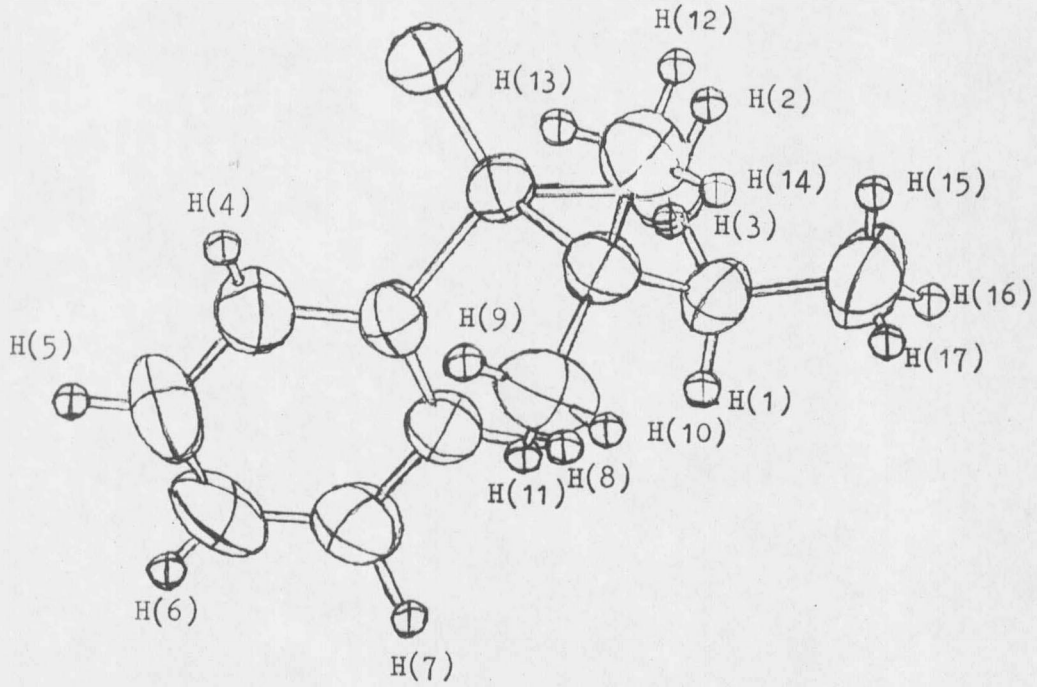

FIGURE III

MOLECULAR STRUCTURE OF
2,2,3-TRIMETHYL-1-PHENYLPHOSPHETANE 1-OXIDE
AT THE 50% PROBABILITY LEVEL (HYDROGENS INCLUDED)

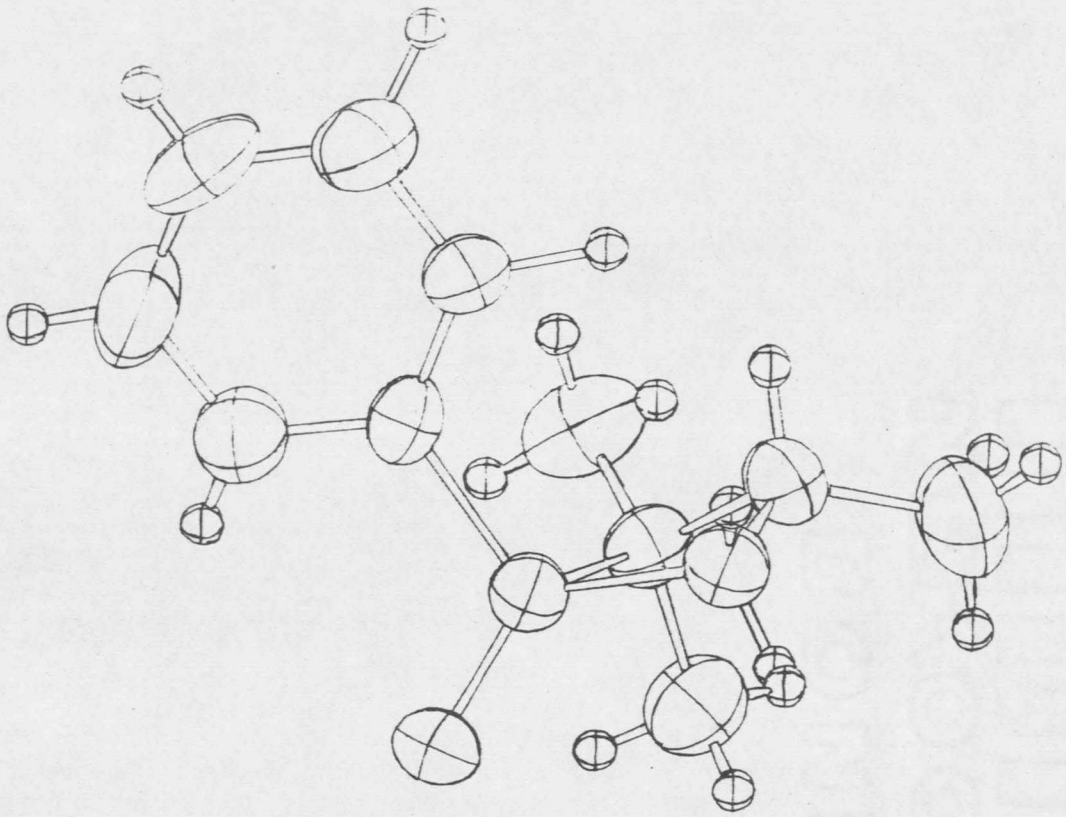

FIGURE IV

ORTEP DRAWING INDICATING THE PUCKER IN THE FOUR-MEMBERED RING

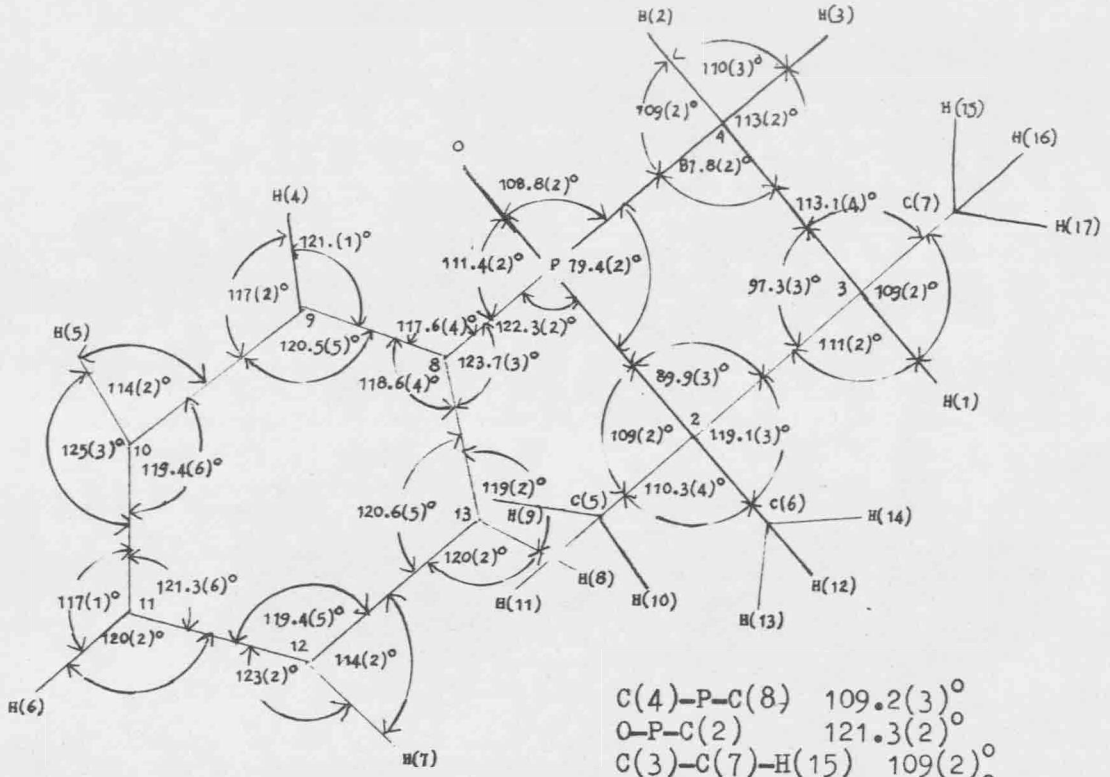

H(12)–C(6)–H(13)	125(6)°
H(12)–C(6)–H(14)	105(5)°
C(2)–C(6)–H(13)	115(3)°
C(2)–C(6)–H(14)	101(3)°

C(4)–P–C(8)	109.2(3)°
O–P–C(2)	121.3(2)°
C(3)–C(7)–H(15)	109(2)°
C(3)–C(7)–H(17)	110(2)°
H(16)–C(7)–H(17)	124(3)°
H(15)–C(5)–H(16)	110(4)°
H(9)–C(5)–H(11)	112(4)°
H(10)–C(5)–H(11)	107(3)°
C(2)–C(5)–H(10)	108(6)°
C(2)–C(5)–H(9)	105(4)°

FIGURE V

BOND ANGLES OF 2,2,3-TRIMETHYL-1-PHENYLPHOSPHETANE 1-OXIDE

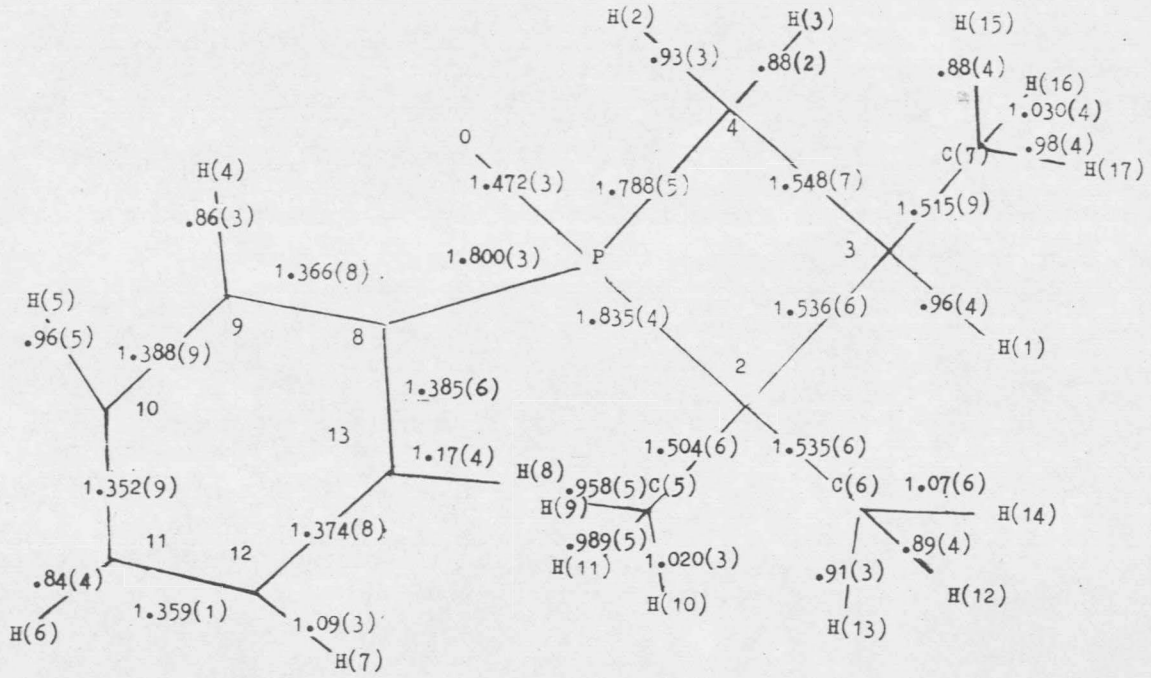

FIGURE VI

BOND DISTANCES FOR 2,2,3-TRIMETHYL-1-PHENYLPHOSPHETANE 1-OXIDE

will be longer than the P–C bond to the more substituted α-carbon. They based this assumption on the ring opening reactions of this class of compounds. In fact, the P–C bond to the least substituted α-carbon is shorter than the P–C bond to the more substituted α-carbon. The previously determined unsymmetrical phosphetane oxide also illustrated this point. The bond distance for the P–C bond to the more substituted α-carbon for that structure was 1.840(5) and the P–C bond to the least substituted α-carbon was 1.799(5). Several authors have attributed the difference in P–C bond lengths in the four-membered ring to the fact that an increased amount of steric interaction would increase the bond distance between two substituted atoms (10–12). Although the argument of steric interactions has been used to explain the difference in bond lengths, it seems unreasonable to assume that this is the reason for the difference in P–C bond lengths in this structure. In a comparison of all the intermolecular distances, it was shown that all of these are well outside the sum of the Van der Waals radii. As a result, the discussion of steric interactions as being responsible for the difference in bond lengths seems invalid for this case. The bond distances and angles are similar to other phosphetane oxides (10–12).

Four-membered rings of this type are expected to be puckered to some degree. A comparison of the amount of ring pucker in the four phosphetane oxides is shown in Figure VII. The angle between the

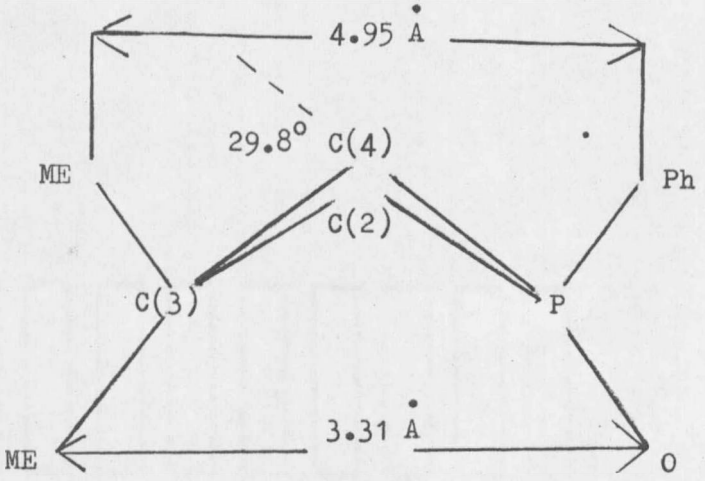

Previous unsymmetrical
phosphetane oxide

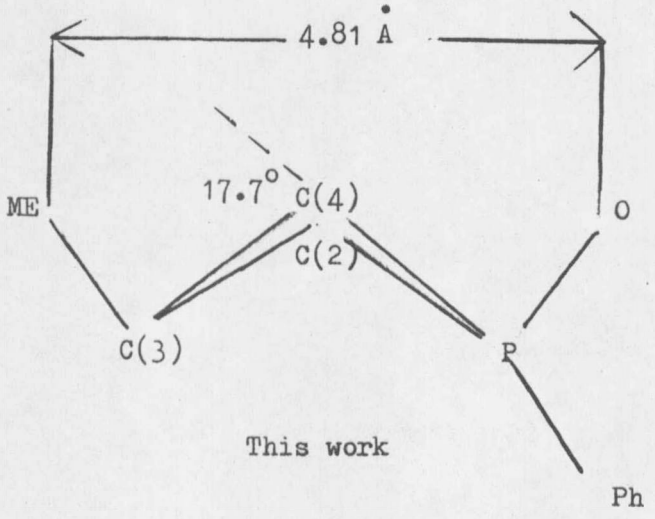

This work

FIGURE VII

COMPARISON OF RING PUCKER IN THE ISOMERIC PHOSPHETANE OXIDES

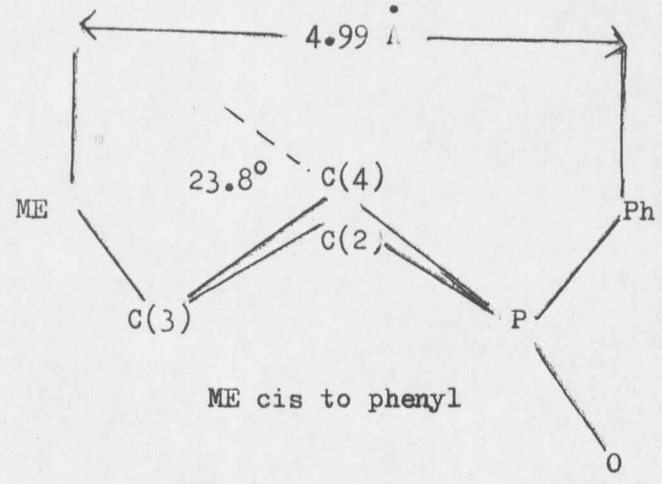

ME cis to phenyl

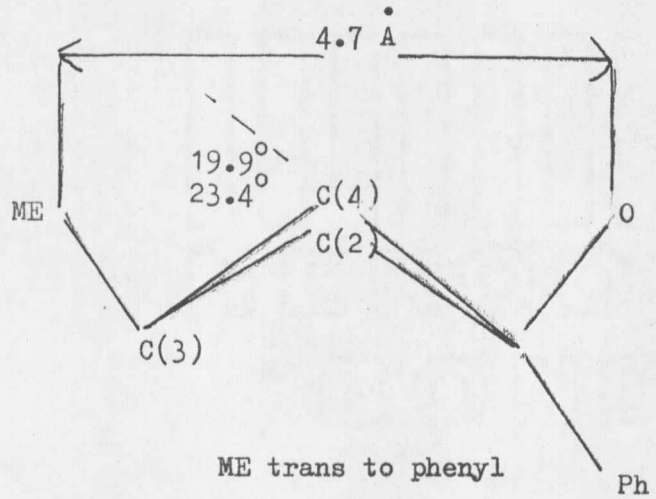

ME trans to phenyl

Two molecules in the asymmetric unit

FIGURE VII (CONTINUED)

planes defined by C(2)-P-C(4) and C(2)-C(3)-C(4) is smaller in this compound than in the other phosphetane oxides.

The phenyl ring is planar with an average displacement of the atoms from the least squares plane of .0058 Å. The maximum displacement from the plane is .0120 Å at the C(11) position. The equations for the various planes of interest are given in Table VI.

A δR plot was constructed for this structure and is shown in Figure VIII (1). To do this, the statistic $\delta R_i = \frac{\Delta F}{\sigma_{F_o}}$ is plotted against the expected error X_i, where X_i is evaluated from the normal probability function

$$P(x) = \frac{1}{\sqrt{2\pi}} \int_{-x}^{x} e^{-\frac{\alpha^2}{2}} \, d\alpha$$

A linear plot with a slope of unity and an intercept of zero indicates that the errors follow a normal distribution and the σ_{F_o} have been correctly estimated. The slope of the least squares line is 1.61 with an intercept of .02 indicating that the σ_{F_o} are underestimated by a factor of about 1.61 and that the distribution of errors follows a normal probability function.

Comparison of the intramolecular bond distances of this structure and the previously determined unsymmetrical phosphetane oxide was

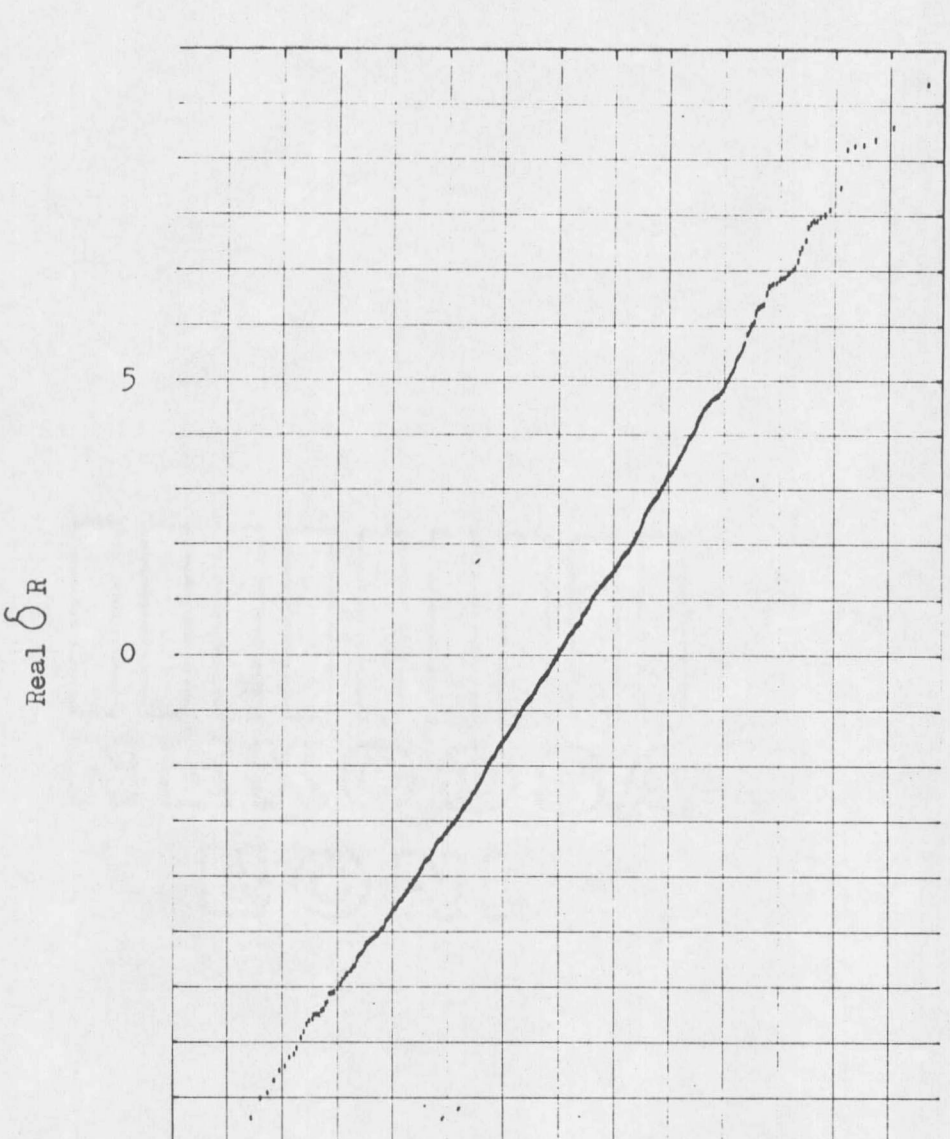

FIGURE VIII

NORMAL PROBABILITY PLOT OF 997 δ_{R_i}; BASED ON F_o

TABLE VI

EQUATIONS OF PLANES[a.] REFERRED TO ORTHOGONAL AXES IN

2,2,3-TRIMETHYL-1-PHENYLPHOSPHETANE 1-OXIDE

ATOMS IN PLANE	l	m	n	b	$S(\Delta^2)$[c.]
C(8), C(9), C(10), C(11), C(12), C(13)	.0851	-.4447	.8916	.6484	.0031
P, C(2), C(4)	.2005	.7754	.5987	2.2476	———
C(2), C(4), C(3)	.5778	.7122	.3986	1.7041	———

(a.) Least squares plane: $lX + mY + nZ - b = 0.0$

(b.) Coordinate system for plane is: X along a, Y in a-b plane, Z along c.

(c.) $S(\Delta)^2$ is the sum of the squares of the deviation of atoms from the planes.

made using a half-normal probability plot (24). The statistic δ_{p_i} is plotted against the expected value of δ_{p_i} which is calculated assuming a normal distribution of errors where

$$\delta_{p_i} = \left| \left| p(1)_i - p(2)_i \right| \Big/ \left(\sigma^2 p(1)_i + \sigma^2 p(2)_i \right)^{\frac{1}{2}} \right.$$

A linear half-normal probability plot with a slope of unity and a zero intercept may generally be interpreted as being due to good agreement between the two structures and correctly estimated standard deviations. The half-normal probability plot is shown in Figure IX for the two unsymmetric phosphetane oxides. The slope of the plot was 4.69 with an intercept of -.778. The bond distances used in the comparison are listed in Table VII and Figure X shows an Ortep drawing of the previously determined unsymmetrical phosphetane oxide for easy referral. The deviation of the slope from unity is probably due to the difference in the amount of pucker in the four-membered rings.

Pseudorotation, that is the interconversion of trigonal bipyramids (1) and (3) by way of the square pyramid (2) which may be a transition state or an intermediate, has been reviewed by Westheimer (30).

TABLE VII

BOND DISTANCES USED IN HALF-NORMAL PROBABILITY PLOT

PREVIOUS WORK		THIS WORK	
ATOMS	BOND DISTANCES	ATOMS	BOND DISTANCES
P-C(2)	1.840(5)[a]	P-C(2)	1.835(4)
P-C(3)	2.360(6)	P-C(3)	2.356(6)
P-C(4)	1.797(4)	P-C(4)	1.788(5)
P-C(7)	3.147(7)	P-C(7)	2.764(5)
P-C(10)	1.820(4)	P-C(8)	1.800(3)
P-C(11)	2.806(6)	P-C(13)	2.816(5)
P-C(12)	4.095(7)	P-C(12)	4.087(6)
P-C(13)	4.561(6)	P-C(11)	4.546(7)
P-C(14)	4.041(6)	P-C(10)	4.029(7)
P-C(15)	2.749(5)	P-C(9)	2.718(6)
P-O	1.477(4)	P-O	1.472(3)

[a] e.s.d's are in parentheses

TABLE VII (CONTINUED)

BOND DISTANCES USED IN HALF-NORMAL PROBABILITY PLOT

PREVIOUS WORK		THIS WORK	
ATOMS	BOND DISTANCES	ATOMS	BOND DISTANCES
C(2)–C(3)	1.584(7)[a]	C(2)–C(3)	1.548(7)
C(2)–C(4)	2.359(7)	C(2)–C(4)	2.315(6)
C(2)–C(7)	2.573(8)	C(2)–C(7)	2.643(9)
C(2)–C(8)	1.515(8)	C(2)–C(6)	1.535(6)
C(2)–C(9)	1.527(8)	C(2)–C(5)	1.504(6)
C(2)–C(10)	3.117(6)	C(2)–C(8)	2.957(7)
C(2)–C(11)	3.726(7)	C(2)–C(13)	3.589(7)
C(2)–C(15)	4.112(7)	C(2)–C(9)	3.889(8)
C(2)–O	2.814(6)	C(2)–O	2.889(5)

[a] e.s.d.'s are in parentheses

TABLE VII (CONTINUED)

BOND DISTANCES USED IN HALF-NORMAL PROBABILITY PLOT

PREVIOUS WORK		THIS WORK	
ATOMS	BOND DISTANCES	ATOMS	BOND DISTANCES
C(3)–C(4)	1.584(7)[a]	C(3)–C(4)	1.536(6)
C(3)–C(7)	1.525(9)	C(3)–C(7)	1.515(9)
C(3)–C(8)	2.640(9)	C(3)–C(5)	2.567(7)
C(3)–C(9)	2.581(8)	C(3)–C(6)	2.579(7)
C(3)–C(10)	3.896(7)	C(3)–C(8)	3.309(7)
C(3)–C(11)	4.348(7)	C(3)–C(13)	3.440(8)
C(3)–O	3.246(6)	C(3)–O	3.649(6)
C(4)–C(7)	2.563(8)	C(4)–C(7)	2.546(8)
C(4)–C(8)	3.665(8)	C(4)–C(5)	3.151(7)
C(4)–C(9)	3.160(7)	C(4)–C(6)	3.612(6)
C(4)–C(10)	3.034(5)	C(4)–C(8)	2.929(7)
C(4)–C(11)	3.412(6)	C(4)–C(13)	3.234(7)
C(4)–C(12)	4.768(8)	C(4)–C(12)	4.595(8)
C(4)–C(15)	4.234(7)	C(4)–C(9)	4.173(8)
C(4)–O	2.802(5)	C(4)–O	2.859(6)

[a] e.s.d's are in parentheses

TABLE VII (CONTINUED)

BOND DISTANCES USED IN HALF-NORMAL PROBABILITY PLOT

PREVIOUS WORK		THIS WORK	
ATOMS	BOND DISTANCES	ATOMS	BOND DISTANCES
C(7)–C(8)	2.882(9)[a]	C(7)–C(5)	2.966(9)
C(7)–C(9)	3.873(8)	C(7)–C(6)	3.564(9)
C(7)–C(10)	4.939(8)	C(7)–C(8)	4.821(9)
C(7)–O	4.745(7)	C(7)–O	4.803(8)
C(8)–C(9)	2.520(9)	C(5)–C(6)	2.494(7)
C(8)–C(10)	4.114(7)	C(5)–C(8)	4.254(7)
C(8)–O	3.169(7)	C(5)–O	3.178(6)
C(9)–C(10)	3.287(7)	C(6)–C(8)	3.250(7)
C(9)–C(11)	3.394(7)	C(6)–C(13)	3.706(7)
C(9)–C(12)	4.521(8)	C(6)–C(12)	4.666(7)
C(9)–C(15)	4.058(7)	C(6)–C(9)	3.903(5)
C(10)–C(11)	1.349(7)	C(8)–C(13)	1.385(6)
C(10)–C(12)	2.382(8)	C(8)–C(12)	2.398(7)
C(10)–C(13)	2.745(7)	C(8)–C(11)	2.748(8)
C(10)–C(14)	2.396(7)	C(8)–C(10)	2.392(9)
C(10)–C(15)	1.397(7)	C(8)–C(9)	1.366(8)
C(10)–O	2.697(6)	C(8)–O	2.711(9)

[a] e.s.d.'s are in parentheses

TABLE VII (CONTINUED)

BOND DISTANCES USED IN HALF-NORMAL PROBABILITY PLOT

PREVIOUS WORK		THIS WORK	
ATOMS	BOND DISTANCES	ATOMS	BOND DISTANCES
C(11)–C(12)	1.387(9)[a]	C(13)–C(12)	1.374(8)
C(11)–C(13)	2.387(8)	C(13)–C(11)	2.360(9)
C(11)–C(14)	2.737(9)	C(13)–C(10)	2.735(9)
C(11)–C(15)	2.369(8)	C(13)–C(9)	2.366(8)
C(11)–O	3.942(7)	C(13)–O	3.966(6)
C(12)–C(13)	1.393(10)	C(12)–C(11)	1.359(10)
C(12)–C(14)	2.370(10)	C(12)–C10)	2,362(9)
C(12)–C(15)	2.746(9)	C(12)–C(9)	2.741(7)
C(13)–C(14)	1.330(10)	C(11)–C(10)	1.352(9)
C(13)–C(15)	2.348(8)	C(11)–C(9)	2.367(7)
C(14)–C(15)	1.373(8)	C(10)–C(9)	1.388(9)
C(14)–O	4.325(7)	C(10)–O	4.401(8)
C(15)–O	2.967(7)	C(9)–O	3.033

[a] e.s.d.'s are in parentheses

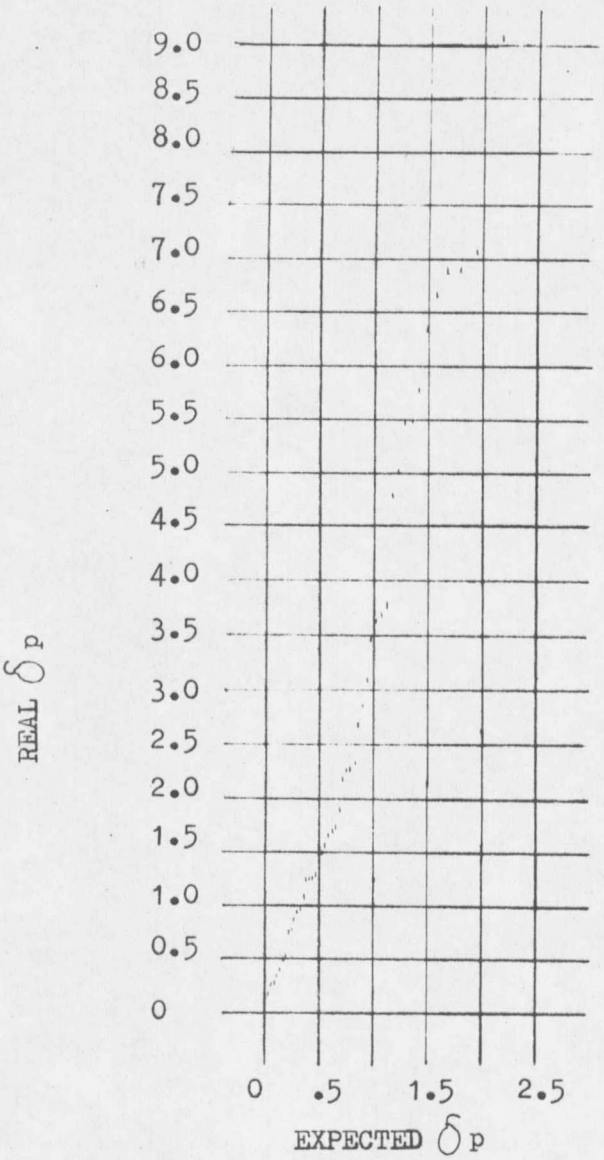

FIGURE IX

HALF-NORMAL PROBABILITY PLOT FOR THE INTRAMOLECULAR DISTANCES EXPECTED TO BE THE SAME IN THE TWO PHENYL PHOSPHETANE OXIDE STRUCTURES

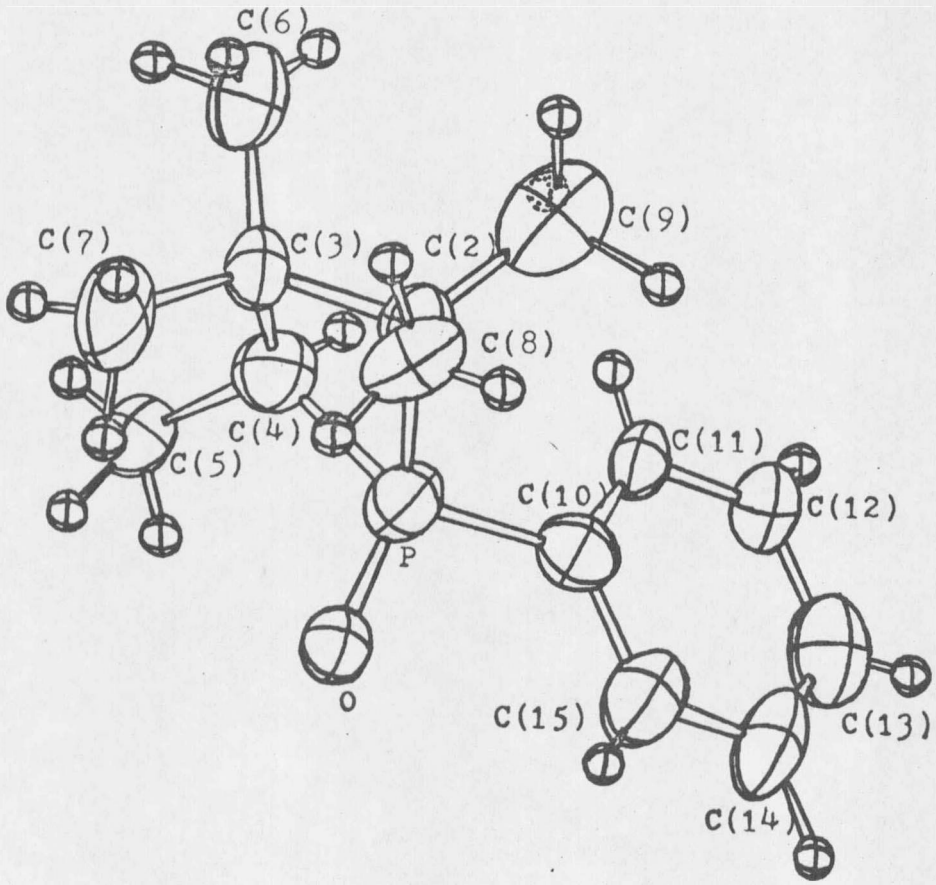

FIGURE X

MOLECULAR STRUCTURE OF

2,2,3,3,4-PENTAMETHYL-1-PHENYLPHOSPHETANE 1-OXIDE

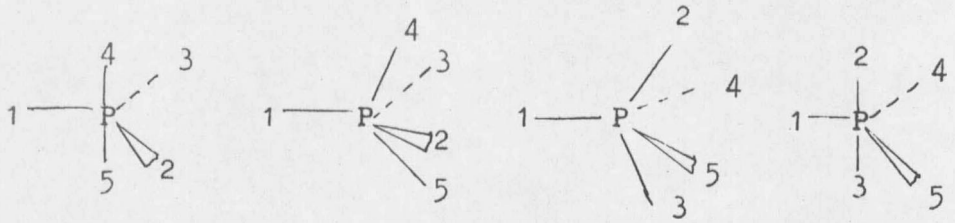

(1) (2) (2) (3)

At the far left, ligands 4 and 5 are apical, and ligands 1,2, and 3 are equatorial; at the far right, ligands 2 and 3 are apical, while 1, 4, and 5 are equatorial. Ligand 1 is the pivot.

Corfield has proposed a trigonal-bipyramid transition state for the basic hydrolysis of the phosphetane oxides in which the ring carbons are axial-equatorial (4). A transition state involving a pseudorotation must be invoked to explain the cleavage of the P-C bond to the least substituted α-carbon. This mechanism is illustrated in Figure XI.

Ezzel suggested that if an intermediate was formed in the cleavage of the phosphetane oxides, the following structure seemed most reasonable (7)

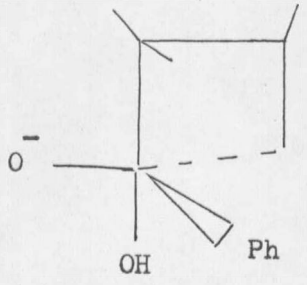

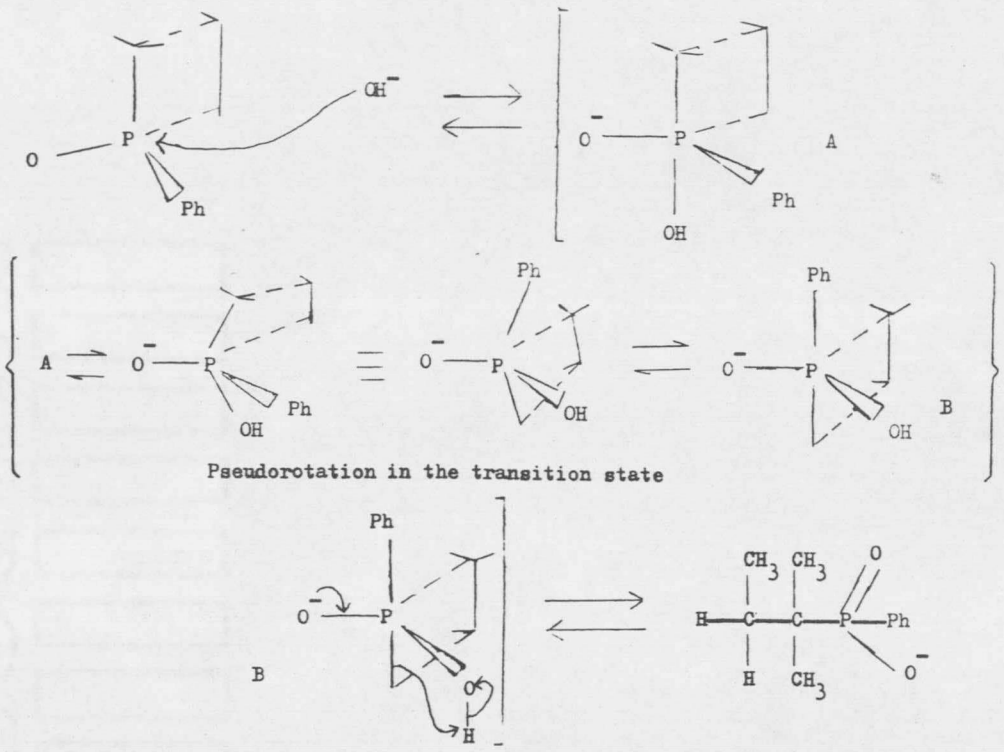

FIGURE XI

MECHANISM FOR THE BASIC HYDROLYSIS OF 2,2,3-TRIMETHYL-1-PHENYLPHOSPHETANE 1-OXIDE

An alternate mechanism for the basic hydrolysis of phosphetane oxides that would lead to cleavage at the least substituted α-carbon was suggested by Dr. Callis. He suggested that if the following compound were used (least substituted α-carbon apical to begin with) no pseudorotation would have to be invoked to explain the cleavage to the least substituted α-carbon.

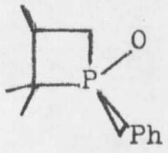

From numerous Ortep drawings and orientations, it was unclear from which direction the OH^- group would attack. It was decided that if the bonds were extended to include the OH^- group, the larger number of interactions would determine the most hindered path of approach. The following figures indicate the extention of the bonds to include the OH^- group. An arbitrary bond distance of 2Å was assigned for the P–O bond distance.

A 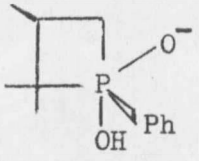

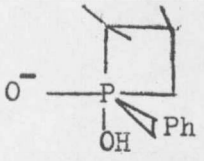

B

From this method, it was found that approach of the OH^- in A led to the larger number of interactions. In A, interactions developed between the OH^- and the oxygen, the carbon in the phenyl group, and the hydrogen on that carbon. The distances obtained were 1.74 Å,

1.94 Å, and 1.38 Å, respectively. In B, the only interaction of any significance was between the OH^- group and the oxygen. The distance was 1.76 Å. Bond distances out to 3Å were examined to determine the number of interactions that the OH^- would encounter when approaching in the direction indicated by the figures A and B.

From this experiment and distances obtained, it was concluded that the mechanism proposed in the thesis actually provides the better starting point (i.e., the approach of the OH^- group is less hindered). The mechanism proposed by Dr. Callis provides not as good a starting point due to hindered approach, but the transition state is proabably better due to the lack of gauche-gauche interactions present in the transition state proposed in the thesis. In order to decide which mechanism would proceed more readily, one would have to determine the differences in energies of the starting points to the transition states to see which mechanism has the lower energy barrier.

It is also postulated that the small interactions between the methyl substituents and the phenyl group has forced the phenyl ring in such a position as to hinder approach of the OH^- group in the mechanism proposed by Dr. Callis.

The four-membered ring occupies apical-equatorial positions and the position-vs.-electronegativity requirements are best satisfied. It seems unreasonable that the coulombic repulsion between the oxide anion and the hydroxide ion would be sufficient to cause deformation of an intermediate with the ring carbons in diequatorial positions.

Mislow has shown that the phosphetane oxides are reduced by hexachlorodisilane and the reaction proceeds with complete retention of configuration at the phosphorus atom (20, 21, 22). This can be explained by the mechanism in Figure XII. Mislow has also done LCAO-MO-SCF calculations on the above system to see if there is an energetically favorable pseudorotation about a specific ligand to account for the retention of configuration. He found that the energy barrier to pseudorotation about ligand 3 (phenyl group) amounts to 2.5 kcal/mole. This is favored over pseudorotation about ligand 2(carbon in the four-membered ring) and about ligand 4 (trichlorosiloxy). The energies for these pseudorotations are 7.1 kcal/mole and 8.7 kcal/mole, respectively. Hence, configuration is retained.

Figure XIII shows a diagram of the four molecules in the unit cell and how they pack together. Figure XIV shows a stereoscopic view of the molecule.

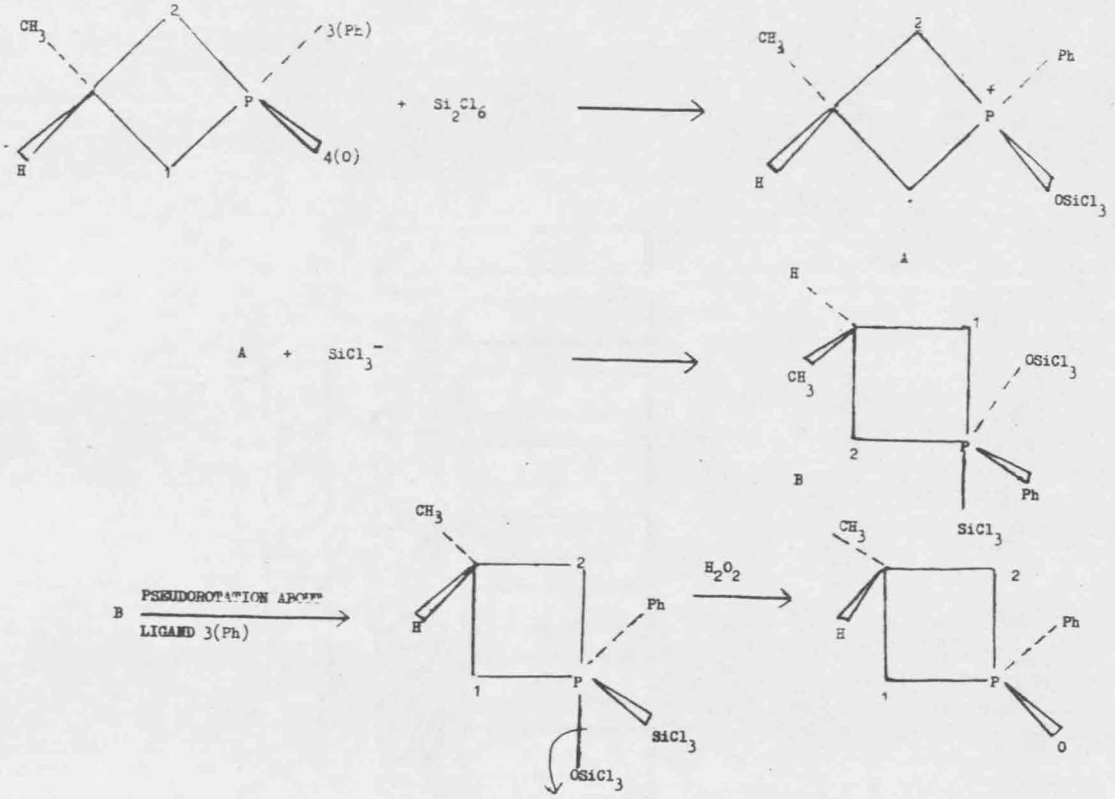

FIGURE XII

MECHANISM FOR THE REDUCTION OF PHOSPHETANE OXIDES WITH HEXACHLORODISILANE

INVOLVING PSEUDOROTATION TO OBSERVE RETENTION OF CONFIGURATION

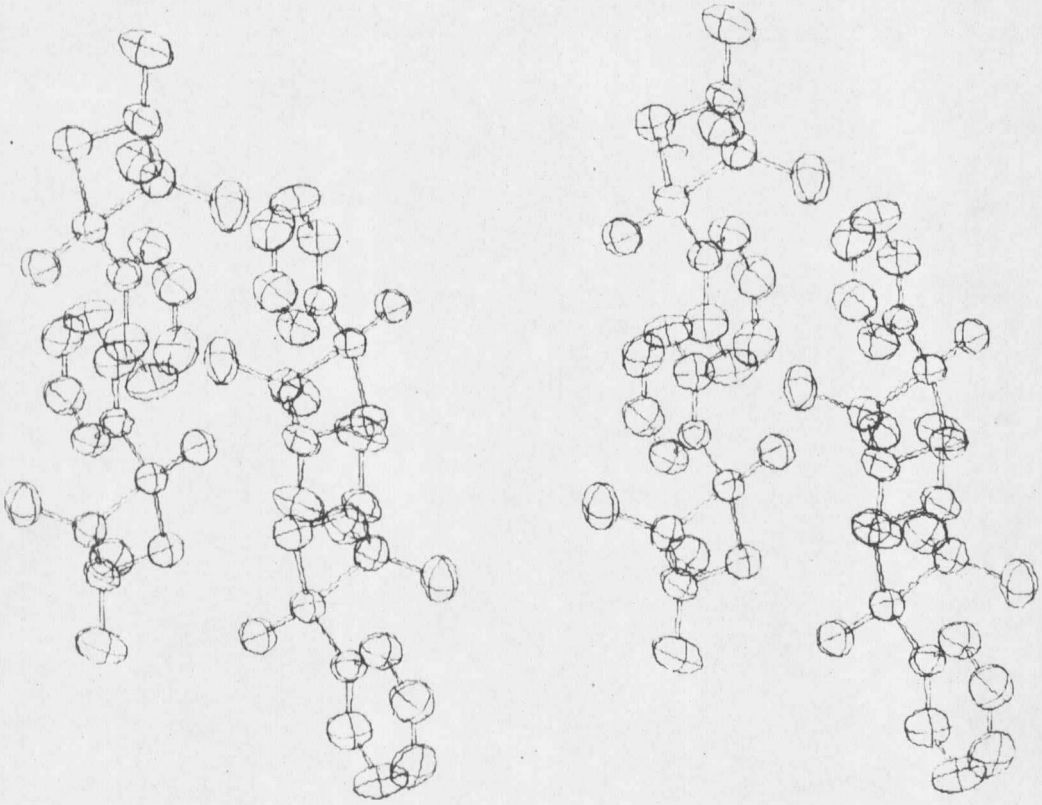

FIGURE XIII

STEREOSCOPIC PACKING DIAGRAM OF

2,2,3-TRIMETHYL-1-PHENYLPHOSPHETANE 1-OXIDE

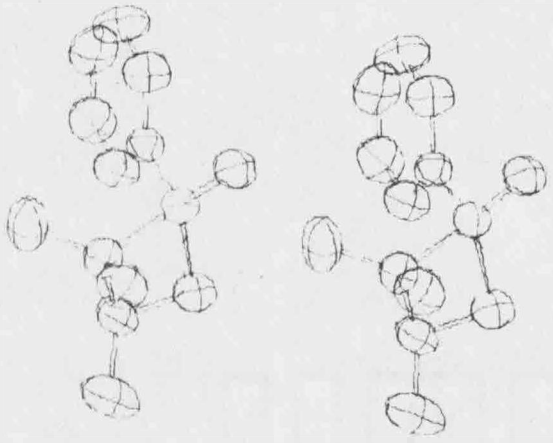

FIGURE XIV

STEREOSCOPIC DIAGRAM FOR 2,2,3-TRIMETHYL-1-PHENYLPHOSPHETANE 1-OXIDE

PART II

2,2,3,4,4-PENTAMETHYL-1-T-BUTYLPHOSPHETANE 1-OXIDE

CHAPTER II

CRYSTAL AND MOLECULAR STRUCTURE OF 2,2,3,4,4-PENTAMETHYL-1-T-BUTYLPHOSPHETANE 1-OXIDE

INTRODUCTION

Originally, the primary purpose for determining the structure of this compound was to correlate structural results with the measured kinetics for pyramidal inversion of the cis⟶ trans geometry (6). Hence, it would be interesting to correlate the rate data with the X-ray work. Originally, the compound would have been the first example of an all aliphatic, solid trivalent phosphine and the first example of a trivalent phosphorus in a four-membered ring. In the original compound, 2,2,3,4,4-pentamethyl-1-t-butyl-phosphetane, the t-butyl and 3-methyl groups were found to be cis by nmr and equilibrium studies.

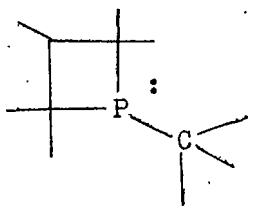

Unfortunately, the structure proved to be the phosphetane oxide and not the phosphetane.

The compound was synthesized by reacting phosphinic acid chloride with t-butyllithium at 0° followed by trichlorosilane reduction of the resultant oxide. Unfortunately, this compound was oxidized by the air and converted to the phosphetane oxide.

The phosphetane was synthesized by Dr. Sheldon Cremer of Marquette University and he kindly supplied the sample.

CHOICE OF CRYSTAL

The solid was recrystallized from a solution of cyclohexane. Two to three weeks were required for crystal growth to occur. Since the crystals turned opaque after prolonged exposure to the atmosphere, the crystal was sealed in a capillary tube for data collection. One of the largest crystals was chosen for the data collection.

The dimensions of the crystal were measured using a calibrated "Whipple disc" in the alignment microscope of the diffractometer. This is done by using the following procedure. The cross-hair reticle in the alignment microscope eyepiece contains a "Whipple disc" which consists of a 10X10 square grid with one grid unit near the center further subdivided into a 5X5 grid. The grid is aligned with one axis lying in the plane of the $\theta - 2\theta$ circle and the other axis normal to this plane. The grid may be calibrated by placing a calibrated scale at the crystal position and observing the image of the scale superimposed on the image of the grid.

The alignment microscope line-of-sight is set normal to the plane of the CHI circle of the single crystal orienter. (This is accomplished with the G.E. XRD-5 diffractometer by setting 2θ at 100.00°.) When CHI and PHI (but not 2θ which is left set at

100.00°) are set for a given reflection, hkl, is viewed as lying parallel to the line-of-sight and normal to the plane of the O-20 circle (i.e., it is viewed as a line parallel to the vertical axis of the grid). Figure XV is a graphical illustration of this situation. Whether the crystal face lies parallel to the line-of-sight can be verified by rotating $\pm$ 10° about PHI and observing that the grazing angle approaches zero as PHI approaches the setting for that reflection.

The indices and the origin-to-face distance for every face, along with the unit cell parameters, constitute the data set necessary to describe the external geometry and dimensions of a single crystal.

Using the procedure described above, the approximate dimensions of the crystal used for the data collection was .882mm X .504mm X .252mm. The linear absorption coefficient for MoK$_\alpha$ radiation was 1.36 cm^{-1}.

DENSITY OF THE COMPOUND

The density of the compound was determined experimentally by the flotation method, using a mixture of ethanol and methyl iodide, that would just suspend the crystal. The experimental density, D_{exp}, is 1.04 g/cc and the calculated density, D_{calc}, based on two molecules

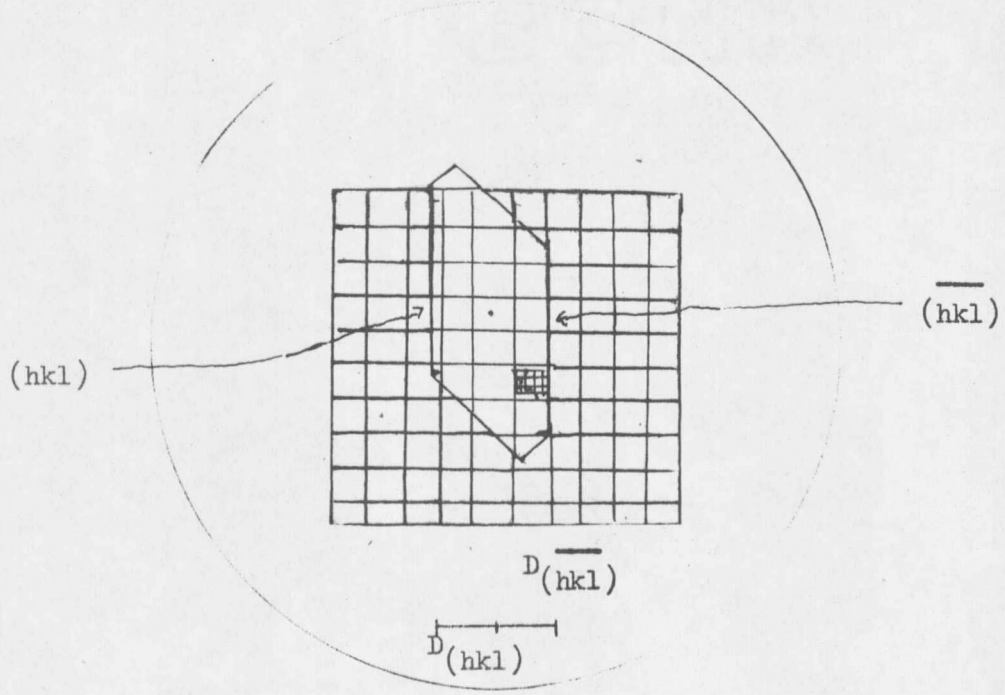

FIGURE XV

GRAPHICAL ILLUSTRATION OF THE VIEW THROUGH THE ALIGNMENT MICROSCOPE OF THE DIFFRACTOMETER SHOWING THE IMAGE OF THE "WHIPPLE DISC" GRID SUPERIMPOSED ON THE IMAGE OF THE CRYSTAL (29)

per unit cell, is 1.05 g/cc.

DETERMINATION OF SPACE GROUP AND CELL DIMENSIONS

A combination of Weissenberg and oscillation photographs showed that the compound crystallized in a monoclinic space group and that the crystal was mounted along the a-axis. The β angle was found from appropriate precession photographs. Approximate cell dimensions obtained from the photographs were $a \cong 6.095$, $b \cong 12.232$, $c \cong 9.122$, and $\beta \cong 96.55^{\circ}$.

From the Weissenberg and precession photographs, the following extinctions were observed:

hkl : no conditions

h0l : no conditions

0k0 : k = 2n

These extinctions do not uniquely determine the space group. Two space groups, $P2_1$ and $P2_1/m$, have the same conditions for reflection. From the measured density and solving for the number of molecules per unit cell, the space group is identified as $P2_1$.

Accurate cell dimensions were determined from a least squares refinement of the 2θ values for twenty independent reflections. Both + 2θ and -2θ values were measured accurately for each reflection and the average 2θ value for the reflection was used in the refinement. The crystal data are listed in Table VIII.

TABLE VIII

2,2,3,4,4-PENTAMETHYL-1-T-BUTYLPHOSPHETANE

1-OXIDE

$C_{12}PH_{25}O$ F.W. = 216.37 F(000)= 240.00

MONOCLINIC, SPACE GROUP $P2_1$

a = 6.133(7) Å

b = 12.174(6) Å

c = 9.047(3) Å

β = 96.42°(3)

Volume of unit cell	671.24 Å^3
Molecules/unit cell	2
Linear absorption Coefficient (μ)	1.36 cm^{-1}
D_{calc}	1.05 g/cc
D_{exp}	1.04 g/cc
λ for MoK_α	.71069 Å

DATA COLLECTION

The intensities of 1314 reflections were measured out to 2θ = to 45°. The method of data collection was the same as in Chapter I. Three standard reflections (013, $\bar{1}40$, 120) were measured a hour intervals throughout the data collection. A scale factor from these was used to scale each block of data to the same scale as the initial block of data. The average value of the scale factor over the entire data set was 1.002 with a standard deviation of .031. This value indicates very little decomposition of the crystal over the course of data collection.

TREATMENT OF THE DATA

The intensities were converted to structure factors ($|F_o|$) using the usual Lorentz-polarization correction for diffractometer data. The weights were calculated for each reflection assuming Poisson counting statistics and an instrumental stability constant of .04 (k_2)

DETERMINATION OF THE STRUCTURE

The structure was solved from the Patterson map and subsequent Fourier maps.

The phosphorus atom positions were easily located from a three-dimensional Patterson map.

For a monoclinic crystal with the b axis designated as the unique axis, the Patterson function is (18)

$$P(UVW) = \frac{4}{V_c} \sum_{0}^{\infty} \sum_{0}^{\infty} \sum_{0}^{\infty} \left(|F(hkl)|^2 \cos 2\pi(hU + lW) + |F(\bar{h}kl)|^2 \cos 2\pi(hU-lW))\cos 2\pi kV \right.$$

For the crystal symmetry $P2_1$, the following equivalent positions exist:

$$x \ , \ y \ , \ z$$

$$\bar{x} \ , \ \tfrac{1}{2} + y \ , \ \bar{z}$$

Considering the vectors between an atom at (x,y,z) and $(\bar{x},\frac{1}{2}+y,\bar{z})$ the following is obtained $u=2x$, $v=\frac{1}{2}$, $w=2z$ indicating that a Harker section exists at $v=\frac{1}{2}$ due to the 2_1 screw axis in the y direction. This peak determines the x and z coordinates of the phosphorus atoms but leaves the y value unspecified. In this space group, however, there is no unique origin point along the b axis, so the y value is assigned arbitrarily.

The atomic coordinates for the phosphorus were determined from the Harker plane. The major peak was found at (.1510, y , .1611). The y coordinate, since it is arbitrary , was given the value of .2500.

A Fourier map was then synthesized to determine the location of all the other atoms.

For the space group $P2_1$, the Fourier expression is (17)

$$\rho(XYZ) = \frac{4}{V_c}\left(\sum_0^\infty \sum_0^\infty \sum_0^\infty \left(|F(hkl)| \cos 2\pi (hX + lZ) \cos 2\pi kY \right.\right.$$

$$\left. + |F(\bar{h}kl)| \cos 2\pi (-hX + lZ) \cos 2\pi kY \right) - \sum_0^\infty \sum_0^\infty \sum_0^\infty \left(|F(hkl)| \right.$$

$$\left.\left. \sin 2\pi (hX + lZ) \sin 2\pi kY + |F(\bar{h}kl)| \sin 2\pi (-hX + lZ) \right| \sin 2\pi kY \right)$$

REFINEMENT

From the first Fourier map, it was possible to locate the atoms of the four-membered ring and the t-butyl group. A problem was encountered from the false symmetry exhibited by this particular space group in the Fourier map. The remaining atomic positions were revealed by three subsequent Fourier maps. R was then 19.8% and the bond angles and bond distances seemed reasonable to start refinement.

Full matrix least squares refinement of the positional and isotropic thermal parameters for the fourteen heavy atoms produced an R value of 14.3%. A series of difference Fourier maps were used to attempt to locate the hydrogen atoms. Not all of the hydrogen atoms were located from several difference maps.

Finally, the positional and individual anisotropic thermal parameters of the fourteen non-hydrogen atoms were refined. After numerous cycles of least squares refinement R was approximately .09.

The anisotropic thermal parameters were then refined along with the isotropic thermal parameters for the fifteen hydrogen atoms. Three cycles of least squares refinement reduced R to .064. Large shifts in the thermal parameters and large standard deviations were still observed at this point of the refinement. As a result, only the gross structure will be reported here.

DISCUSSION OF THE STRUCTURE

The positional parameters of the non-hydrogen atoms are listed in Table IX. Figure XVI is an Ortep drawing of the structure with the ellipsoids calculated at the 50% probability level(19). The bond angles and bond distances are presented in Figure XVII and Figure XVIII.

The bond angles and bond distances are comparable to a symmetrical phosphetane oxide done earlier(11). In this structure, there were large standard deviations in the atomic positions as well as the bond distances. The long C-C bond distances in certain bonds, in this structure as well as the one above, may reflect the strain in the four-membered ring.

At the time of this writing, an attempt is being made to recollect another set of data that hopefully will lead to a better structure.

TABLE IX

POSITIONAL PARAMETERS FOR THE NON-HYDROGEN ATOMS IN 2,2,3,4,4-PENTAMETHYL-1-T-BUTYLPHOSPHETANE 1-OXIDE

ATOM	x/a	y/b	z/c
P	.14773	.25000	.15741
C(2)	.3122	.1538	.2819
C(3)	.4554	.2504	.3429
C(4)	.3148	.3496	.2823
C(5)	.4449	.4392	.2221
C(6)	.4187	.0558	.2101
C(7)	.1463	.1163	.4027
C(8)	.1602	.4011	.3849
C(9)	.5419	.2603	.5079
C(10)	.0786	.1503	-.1037
C(11)	.4482	.2562	-.0633
C(12)	.2048	.2529	-.0374
C(13)	.0974	.3581	-.1172
C(14)	-.0929	.2519	.1612

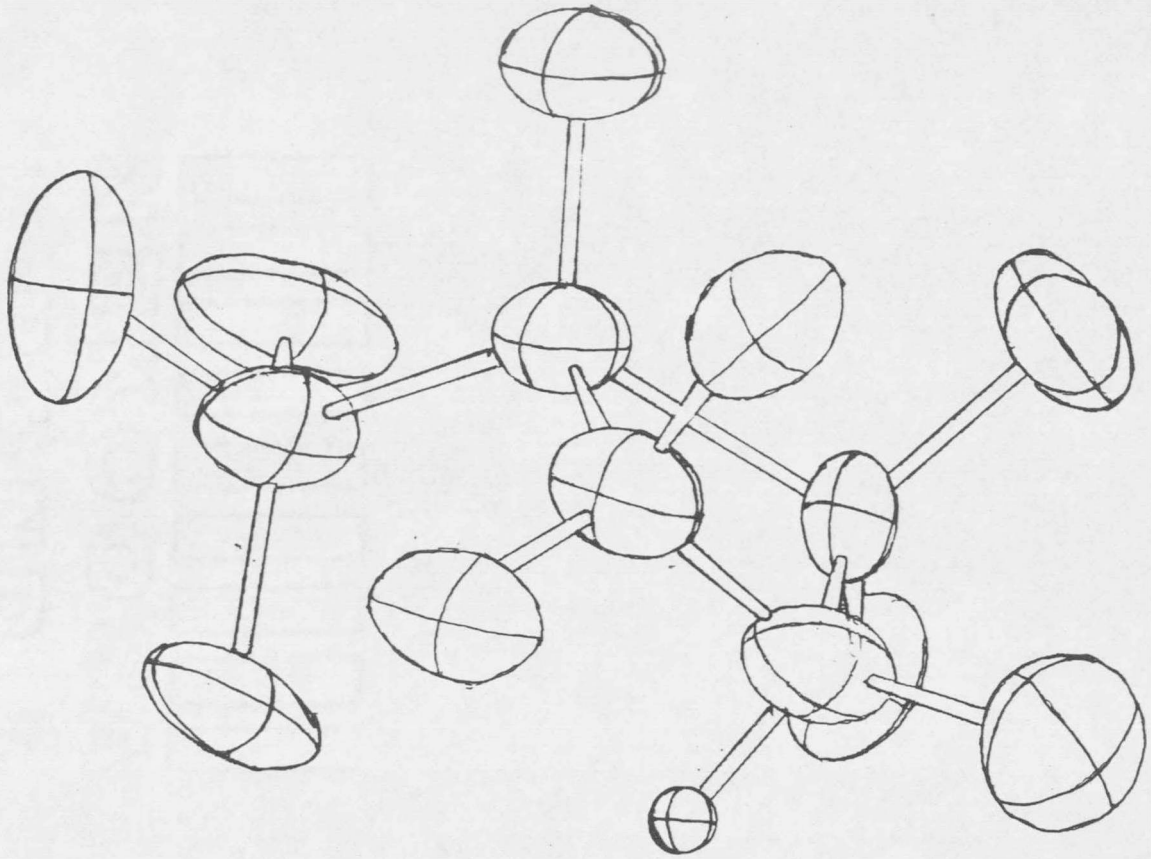

FIGURE XVI

ORTEP DRAWING FOR 2,2,3,4,4-PENTAMETHYL-1-T-BUTYLPHOSPHETANE 1-OXIDE

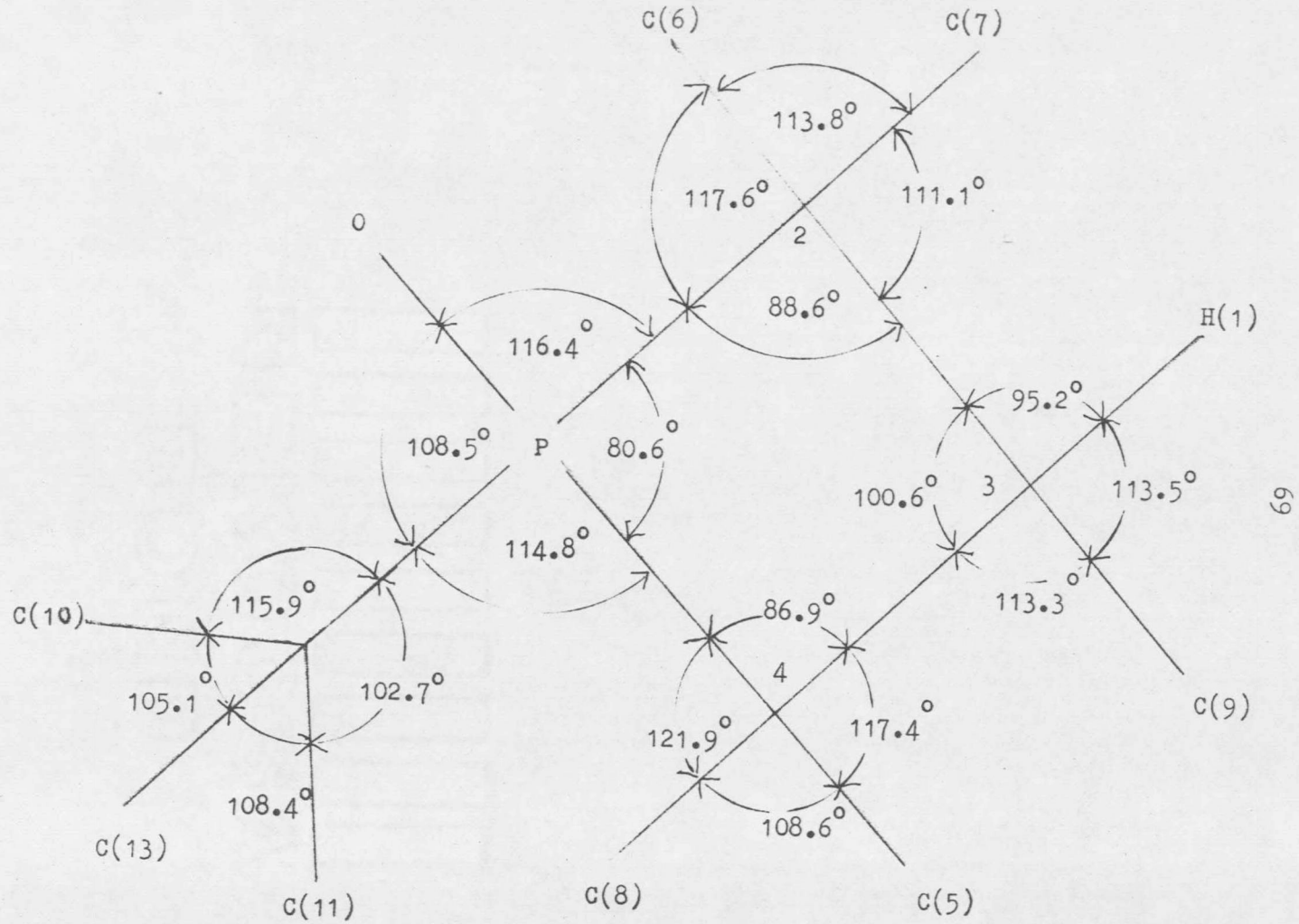

FIGURE XVII

BOND ANGLES FOR 2,2,3,4,4-PENTAMETHYL-1-T-BUTYLPHOSPHETANE 1-OXIDE

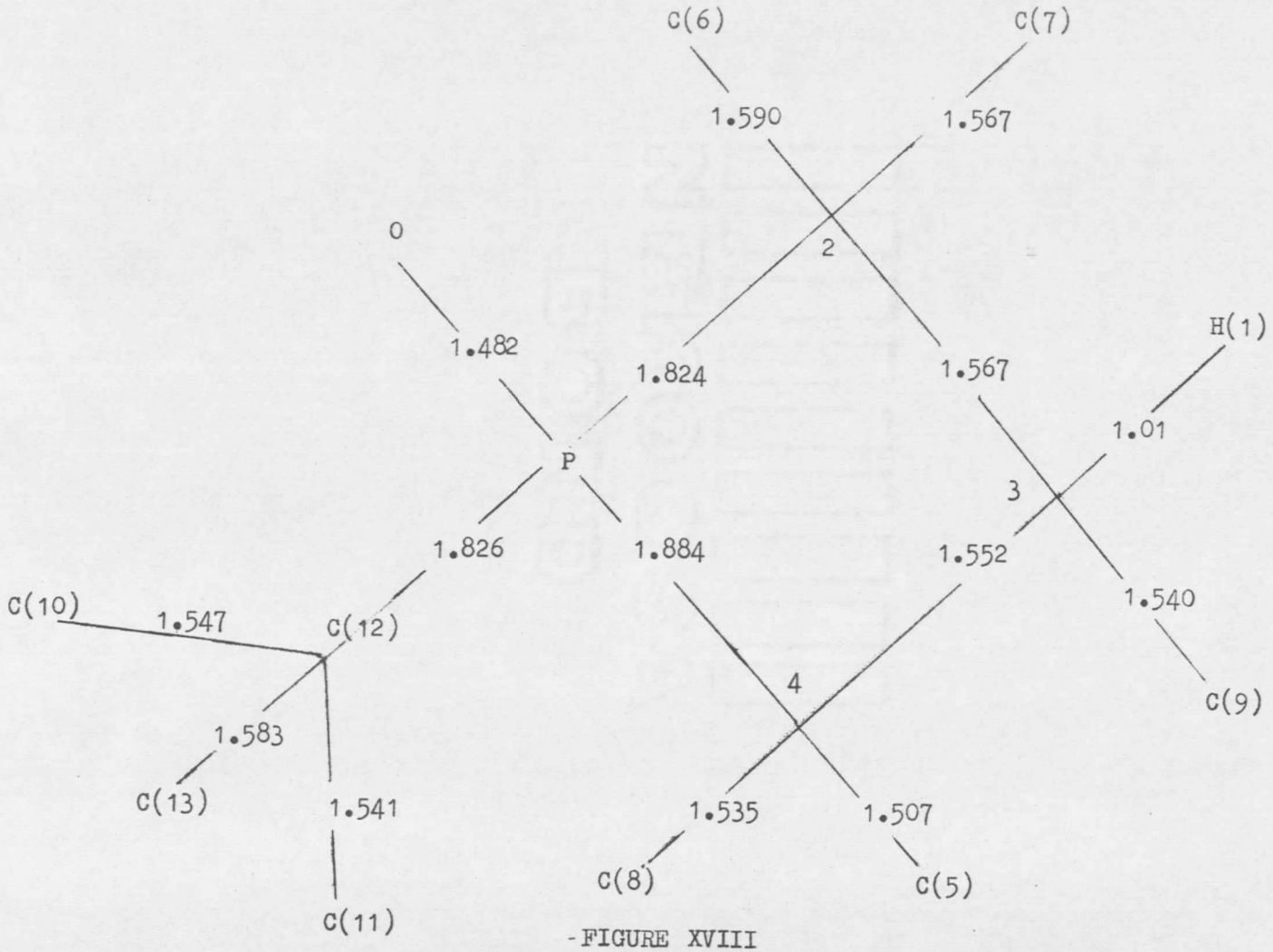

-FIGURE XVIII

BOND DISTANCES FOR 2,2,3,4,4-PENTAMETHYL-1-T-BUTYLPHOSPHETANE 1-OXIDE

CHAPTER III

SUMMARY AND CONCLUSIONS

The three-dimensional structure of 2,2,3-trimethyl-1-phenyl-phosphetane 1-oxide has been determined. This represents only the second unsymmetrical phosphetane oxide whose structure has been determined. The single methyl group is trans to the phenyl group. The P-C bond to the least substituted α-carbon is significantly different (shorter) than the other P-C bond. This result is in opposition to the predicted bond lengths based on ring opening reactions (23). A reaction mechanism for the basic hydrolysis of this type of compound has been proposed. The reaction mechanism is consistent with both the increased reactivity of the less highly substituted compounds and the observed products. The proposed transition state involves a pseudorotation from an initial activated complex, A, to a more stable activated complex, B. The axial-equatorial arrangement of the two oxygen atoms in the trigonal-bipyramid of A is less stable than the equatorial-equatorial arrangement of the atoms in B. This may be used to explain the observed cleavage of the P-C bond to the least substituted α-carbon. A mechanism has also been proposed for the reduction of phosphetane oxides with hexachlorodisilane. This mechanism is consistent with the

observed results of retention of configuration.

The structure of 2,2,3,4,4-pentamethyl-1-t-butylphosphetane 1-oxide is not fully completed. As a result, only the gross structure has been reported.

BIBLIOGRAPHY

1. Abrahams, S. C., and Keve, E. T., (1971). Acta Cryst., A27, 157.

2. Buerger, M. J., (1959). "Vector Space". Wiley, New York. Pages 5-59, 41-64.

3. Busing, W. R., and Levy, H. A., (1959). "A Crystallographic Least Squares Program for the IBM 704",ORNL 59-4-37. Oak Ridge National Laboratory, Tenn. As modified for use in the Montana State University Crystallographic Library of Programs.

4. Corfield, J. R., Harger, M. J. P., Shutt,J. R., and Triplett, S., (1970). J. Chem. Soc.,(C), 1855.

5. Cremer, S. E., and Chorvat, R. J., (1967). J. Org. Chem., 32, 4066.

6. Cremer, S. E., Chorvat, R. J., Chang, C.H., and Davis, D. W., (1968). Tetrahedron Letters, 5799.

7. Ezzel, B. R., (1970). J. Org. Chem., 35, 2426.

8. Ezzel, B. R., and Freedman, L. D., (1970). J. Org. Chem., 35, 241.

9. Ezzel, B. R., and Freedman, L. D., (1969). J. Org. Chem., 34, 1777.

10. Fitzgerald, A., (1973). Ph.D. Thesis, Montana State University.

11. Haque, M. U., (1970). J. Chem. Soc., (B), 938.

12. Haque, M. U., (1971). J. Chem. Soc., (B), 117.

13. Hamilton, W. C., (1965). Acta. Cryst., 18, 502.

14. Horner, L., and Blazer, W. E., (1965). Tetrahedron Letters, 1157.

15. International Tables for X-ray Crystallography, (1962). Vol. I, Tables, 3.31A, 3.32C, 5.35B. Kynoch, Birmingham, England.

16. International Tables for X-ray Crystallography, (1962). Vol. I, page 383. Kynoch, Birmingham, England.

17. International Tables for X-Ray Crystallography, (1962). Vol. I, page 375. Kynoch, Birmingham, England.

18. International Tables for X-Ray Crystallography, (1962). Vol. I, page 526. Kynoch, Birmingham, England.

19. Johnson, C. K., (1965). "Ortep: A Fortran Thermal Ellipsoid Plot Program for Crystal Structure Illustrations", ORNL-3794. Oak Ridge National Laboratory, Tenn.

20. Mislow, K., DeBruin, K. E., Naumann, K., and Zon, G., (1969). J. Am. Chem. Soc., 91, 7031.

21. Mislow, K., DeBruin, K. E., Naumann, K., and Zon, G., (1969). J. Am. Chem. Soc., 91, 7027.

22. Mislow, K., Naumann, K., and Zon, G., (1969). J. Am. Chem. Soc., 91, 7012.

23. Moret, C., and Trefonas, L. M., (1969). J. Am. Chem. Soc., 91, 2255.

24. Smith, G. D., (1973). Progress for Evaluation of Both Normal and Half-Normal Probability Functions and for Plotting the Data. Montana State University Crystallographic Library of Programs.

25. Stewart, R. F., Davidson, D. R., and Simpson, W. T., (1965). J. Chem. Phys., 42, 3175.

26. Stout, G. H., and Jensen, L. H., (1968). "X-Ray Structure Determination". MacMillan, New York. Pages 212-238.

27. Stout, G. H., and Jensen, L. H., (1968). "X-Ray Structure Determination". MacMillan, New York. Page 457.

28. Stout, G. H., and Jensen, L. H., (1968). "X-Ray Structure Determination". MacMillan, New York. Page 196.

29. Ward, D. L., (1972). Ph.D. Thesis, Montana State University.

30. Westheimer, F. H., (1968). Accounts of Chem. Res., 1, 70.

Campbell, James Allen
Crystal and molecular structure of phosphetane oxides